

Tabular Foundation Models Can Do Survival Analysis

Da In Kim ^{*1} Wei Siang Lai ^{*2} Kelly W. Zhang ²

Abstract

While tabular foundation models have achieved remarkable success in classification and regression, adapting them to model time-to-event outcomes for survival analysis is non-trivial due to right-censoring, where data observations may end before the event occurs. We develop a classification-based framework that reformulates both static and dynamic survival analysis as a series of binary classification problems by discretizing event times. Censored observations are naturally handled as examples with missing labels at certain time points. This classification formulation enables existing tabular foundation models to perform survival analysis through in-context learning without explicit training. We prove that under standard censoring assumptions, minimizing our binary classification loss recovers the true survival probabilities as the training set size increases. We demonstrate through evaluation across 53 real-world datasets that off-the-shelf tabular foundation models with this classification formulation outperform classical and deep learning baselines on average over multiple survival metrics.

1. Introduction

Survival analysis or time-to-event analysis models *when* an event of interest will occur, rather than just *whether* it will happen or not (Wang et al., 2019). Applications of survival analysis span many domains, including healthcare (e.g., time to disease recurrence or mortality), social sciences (e.g., duration of unemployment), engineering (e.g., time to equipment failure), and finance/business (e.g., time to default or until a customer churns).

A defining feature of survival analysis that differentiates it from standard regression is censoring, where the true event time is only partially observed (Klein & Moeschberger, 2006). Under right-censoring, the exact time an event of

interest occurs may be unknown because the observation period may end before the event happens. For example, consider a 5-year clinical drug trial where mortality is the main outcome; the mortality event may be right-censored if the individual drops out early or remains alive through the 5-year observation period. This incomplete event time information distinguishes survival analysis from standard regression tasks, where the target is always observed.

Despite its broad applicability, survival analysis often remains challenging due to (a) right-censoring, (b) small dataset sizes, e.g., a several hundred samples or fewer (Drysdale, 2022), and (c) covariates that may be irregularly sampled over time (Wang et al., 2019). While foundation models have been developed for survival analysis in specialized medical tasks (Steinberg et al., 2024; Vu et al., 2025), for general-purpose survival analysis, it remains standard to use specialized models fit from scratch on a single dataset, without the use of pretrained representations. Recent work has investigated the ability of large language models for survival analysis, primarily through prompting or few-shot learning (Jeanselme et al., 2024); these approaches have been used primarily in narrowly defined clinical settings, e.g., cancer prognosis or cardiovascular risk (Hu et al., 2024; Han et al., 2023), and do not explicitly address how to learn from censored data.

Recently, tabular foundation models (TFMs) (Hollmann et al., 2023; Grinsztajn et al., 2025; Zhang et al., 2025; Gardner et al., 2024) have achieved remarkable success in classification and regression tasks, often outperforming methods like XGBoost, especially in small-data regimes. TFM are usually transformer-based models, pretrained on a diverse collection of synthetic or real-world datasets, that are able to perform in-context learning at inference time without parameter updates. While this paradigm offers a promising direction for survival analysis, adapting TFM to this setting is non-trivial. Standard regression architectures cannot easily account for censoring, a challenge that historically necessitated the development of specialized variants for survival analysis, e.g., Random Survival Forest (Ishwaran et al., 2008). Additionally, while TFM are primarily evaluated on classification accuracy or mean squared error, survival modeling requires well-calibrated probabilities that accurately characterize risk dynamics over time.

¹Department of Computing, Imperial College London

²Department of Mathematics, Imperial College London. Correspondence to: Kelly W. Zhang <kelly.zhang@imperial.ac.uk>.

Contributions. In this work, we cast survival analysis as a series of binary classification problems, which allows us to leverage existing TFM classifiers for in-context learning for survival analysis. Our approach discretizes event times, a common practice in the survival analysis literature (Efron, 1988; Craig et al., 2025; Allison, 1982; Singer & Willett, 1993; Lee et al., 2019; Yu et al., 2011; Maystre & Russo, 2022), and is applicable to both static and dynamic survival modeling. Our contributions are as follows:

(1) Classification formulation of survival analysis. By reformulating survival analysis into a binary classification problem, survival models can be optimized using a standard binary cross-entropy loss. This framework enables TFM classifiers to perform survival analysis out-of-the-box via in-context learning, leveraging pretrained representations to achieve high performance without requiring additional model training or hyperparameter tuning.

(2) Consistent model guarantee as the training set grows. We prove that minimizing our binary cross-entropy loss recovers the true underlying survival probabilities as the training sample size grows. This consistency result holds under a conditional independent censoring assumption that is common in the survival analysis literature (Uno et al., 2011; Kalbfleisch & Prentice, 2002). We also show empirically that classification models with lower binary cross-entropy loss have more accurate survival probabilities (Figure 3).

(3) Empirical evaluation on a suite of real-world survival analysis datasets. We evaluate on 43 static and 5 dynamic real-world survival analysis datasets from *SurvSet* (Drysdale, 2022). We find that TFM, using our classification framework, outperform a variety of classical and deep learning-based survival models on average across multiple common survival metrics.

2. Problem statement

We consider both *static* and *dynamic* survival analysis settings (Chen et al., 2024; Van Houwelingen & Putter, 2011). While the static survival analysis models event times given baseline features collected at the start of observation, dynamic models incorporate longitudinal data, updating predictions as more information becomes available.

2.1. Static setting

Each dataset consists of a collection of n i.i.d. data tuples $\{(X_{i,0}, T_i, C_i, \delta_i)\}_{i=1}^n$. Here, $X_{i,0} \in \mathbb{R}^d$ is a feature vector consisting of baseline covariates given at the start of the observation period. $T_i > 0$ represents the (latent) event time and $C_i > 0$ is the censoring time. We use $\delta_i \triangleq \mathbb{1}(T_i \leq C_i)$ as an indicator of whether the event is observed or censored. Note, $\delta_i = 1$ if the event is observed and $\delta_i = 0$ if censored.

Our primary objective is to estimate the survival probability $S(t | X_{i,0})$, which represents the probability that the event occurs after time t :

$$S(t | X_{i,0}) \triangleq \mathbb{P}(T_i > t | X_{i,0}). \quad (1)$$

Note that $S(t | X_{i,0})$ is a monotonically decreasing function of t with $S(0 | X_{i,0}) = 1$ and $\lim_{t \rightarrow \infty} S(t | X_{i,0}) = 0$.

Next, we introduce a conditionally independent censoring assumption. Note, without this assumption, the survival probabilities are provably not identifiable from observed data (Tsiatis, 1975).

Assumption 2.1 (Conditionally Independent Censoring). The event time T_i and censoring time C_i are conditionally independent given $X_{i,0}$, i.e., $T_i \perp\!\!\!\perp C_i | X_{i,0}$.

2.2. Dynamic setting

In the dynamic setting, the baseline covariate vector $X_{i,0}$ is replaced by a sequence of observations revealed over time. These covariates can be observed at irregular intervals. We denote this sequence of covariates as $\mathcal{X}_i \triangleq \{X_{i,t} : t \in \mathcal{T}_i\}$, where $\mathcal{T}_i \subset [0, \infty)$ represents the observation times. The history of covariates up to time t is defined as

$$\mathcal{H}_{i,t} \triangleq \{(s, X_{i,s}) : s \in \mathcal{T}_i, s \leq t\}. \quad (2)$$

Consistent with the static setting, the dataset contains n i.i.d. tuples $\{(\mathcal{X}_i, T_i, C_i, \delta_i)\}_{i=1}^n$, where the definitions of T_i , C_i , and δ_i follow Section 2.1.

The modeling task is to estimate the conditional survival probability for a future horizon $\Delta > 0$, given the information available at time t :

$$S(t + \Delta | T_i > t, \mathcal{H}_{i,t}) \triangleq \mathbb{P}(T_i > t + \Delta | T_i > t, \mathcal{H}_{i,t}). \quad (3)$$

We use a dynamic analogue of the conditionally independent censoring condition from the static setting (Assumption 2.1), which helps ensure the dynamic survival probabilities (3) are identifiable from observed longitudinal data.

Assumption 2.2 (Dynamic Conditionally Independent Censoring). For any $t \geq 0$, the event time T_i and censoring time C_i are conditionally independent given the history and survival up to time t , i.e., $T_i \perp\!\!\!\perp C_i | (\mathcal{H}_{i,t}, T_i > t)$.

3. Methodology: Time-to-event modeling as supervised learning

We frame survival modeling under right-censoring as a series of binary classification tasks. By reducing survival modeling to a standard classification task, we can leverage the tabular foundation models and enable survival modeling via in-context learning without additional survival-specific

training or hyperparameter tuning. Our approach involves transforming each time-to-event data tuple into a sequence of binary labels indicating whether the event has occurred by the end of each respective time interval. We first describe our temporal discretization approach, as it underpins the classification formulations for both the static (Section 3.1) and dynamic (Section 3.2) settings.

Temporal discretization. To transform the continuous survival task into a tractable classification problem, we partition the time horizon into K discrete intervals $\{\tau_k\}_{k=1}^K$. Given the boundaries $0 = t_0 < t_1 < t_2 < \dots < t_{K-1}$, we define the intervals as $\tau_k = (t_{k-1}, t_k]$ for $k < K$, with a final open-ended interval $\tau_K = (t_{K-1}, \infty)$. For convenience, let $t_K \triangleq \infty$. In practice, we determine the boundaries $\{t_k\}_{k=1}^{K-1}$ using the quantiles of the observed event times in the training set to ensure a balanced distribution of events across intervals. This time discretization approach is well-established in the survival analysis literature (Efron, 1988; Craig et al., 2025; Allison, 1982; Singer & Willett, 1993; Lee et al., 2019; Yu et al., 2011; Maystre & Russo, 2022).

3.1. Static setting

Constructing the supervised learning dataset. To transform survival modeling into a supervised learning problem, we define binary labels $\{Y_{i,k}\}_{k=1}^{K-1}$ where

$$Y_{i,k} \triangleq \mathbb{1}(T_i \leq t_k). \quad (4)$$

Note, we do not define $Y_{i,K}$ since $t_K \triangleq \infty$ implies $\mathbb{1}(T_i \leq t_K) = 1$ almost surely. Due to right-censoring, $Y_{i,k}$ is only observed when $t_k < C_i$. Note that by construction $T_i \in \tau_k$ for some interval τ_k where $k \in [1: K-1]$, since $T_i < \infty$. Figure 1 illustrates this process.

The original time-to-event data tuple $(X_{i,0}, T_i, C_i, \delta_i)$ is expanded into $K-1$ data tuples for binary classification:

$$\{((X_{i,0}, t_k), Y_{i,k}, C_i)\}_{k=1}^{K-1}.$$

The censoring time C_i above will be used to derive whether the label $Y_{i,k}$ is observed or missing for the time interval τ_k .

Model training. We train a classifier \hat{p} to minimize a empirical binary cross-entropy loss; below, the indicator $\mathbb{1}(t_k < C_i)$ restricts the objective to observed labels $Y_{i,k}$:

$$\hat{\ell}_{\text{static}}(\hat{p}) \triangleq \frac{1}{n} \sum_{i=1}^n \sum_{k=1}^{K-1} \mathbb{1}(t_k < C_i) \cdot \text{BCE}(\hat{p}(X_{i,0}, t_k), Y_{i,k}) \quad (5)$$

where

$$\text{BCE}(p, Y) \triangleq -\{Y \log p + (1 - Y) \log(1 - p)\}. \quad (6)$$

By only evaluating the loss only for pairs (i, t_k) where $t_k < C_i$, we restrict training strictly to observed labels

$Y_{i,k}$. While simply ignoring unobserved data might appear to be a heuristic handling of censoring, we formally show in Section 3.3 that minimizing this loss recovers the true underlying survival probabilities as $n \rightarrow \infty$.

The cross-entropy loss from (5) can be minimized using standard classification models, such as XGBoost or multi-layer perceptrons. Furthermore, this framework allows us to “fit” \hat{p} via in-context learning using tabular foundation models for classification (Hollmann et al., 2023; Zhang et al., 2025), where \hat{p} is computed by conditioning on the set of tuples $((X_{i,0}, t_k), Y_{i,k})$ for which $t_k < C_i$.

Inference. Given a binary classifier \hat{p} , we form our estimate of the survival probability $S(t_k | X_{i,0})$ as follows:

$$\hat{S}(t_k | X_{i,0}) \triangleq 1 - \hat{p}(X_{i,0}, t_k). \quad (7)$$

To ensure the survival probabilities are monotonically decreasing in t_k , by clipping $1 - \hat{p}(X_{i,0}, t_k)$ if it is larger than $1 - \hat{p}(X_{i,0}, t_{k-1})$. See Appendix C.1.1 for details.

3.2. Dynamic setting

We adopt the same temporal discretization and binary label definition, $Y_{i,k} \triangleq \mathbb{1}(T_i \leq t_k)$, as in the static setting. In the dynamic setting, however, the model must account for time-varying information. At a given timestep t_k , the model is provided with the covariate history $\mathcal{H}_{i,t_k} \triangleq \{(s, X_{i,s}) : s \in \mathcal{T}_i, s \leq t_k\}$ and the knowledge that the subject has survived up to t_k (i.e., $Y_{i,1} = \dots = Y_{i,k} = 0$).

Consequently, each original time-to-event data tuple $(\mathcal{X}_i, T_i, C_i, \delta_i)$ is transformed into training examples:

$$((\mathcal{H}_{i,t_k}, Y_{i,1:k}, t_k, t_{k+\Delta}), Y_{i,k+\Delta}, C_i),$$

for each $k \in \{0, \dots, K-2\}$ and $\Delta \in \{1, \dots, K-k-1\}$, provided $t_k < C_i$. We use $Y_{i,1:k} \triangleq (Y_{i,1}, \dots, Y_{i,k})$. Same as in the static setting, C_i is used to derive whether the $Y_{i,k+\Delta}$ is observed or missing.

Model training. We train a binary classifier \hat{p} to minimize the dynamic empirical binary cross-entropy loss:

$$\begin{aligned} \hat{\ell}_{\text{dynamic}}(\hat{p}) &\triangleq \frac{1}{n} \sum_{i=1}^n \sum_{k=0}^{K-2} \sum_{\Delta=1}^{K-k-1} \mathbb{1}(t_k < T_i) \mathbb{1}(t_{k+\Delta} < C_i) \\ &\quad \times \text{BCE}(\hat{p}(\mathcal{H}_{i,t_k}, Y_{i,1:k}, t_k, t_{k+\Delta}), Y_{i,k+\Delta}). \end{aligned} \quad (8)$$

We include the indicator $\mathbb{1}(t_k < T_i)$ to ensure that we only train on examples for which the event is at risk, i.e., if the event occurred before time t_k , we are not using \mathcal{H}_{i,t_k} to do further prediction. Similar to the static setting, the indicator $\mathbb{1}(t_{k+\Delta} < C_i)$ to account for censoring effectively truncates the label sequence $Y_{i,1:K}$; our formulation allows us to utilize all information prior to that truncation time.

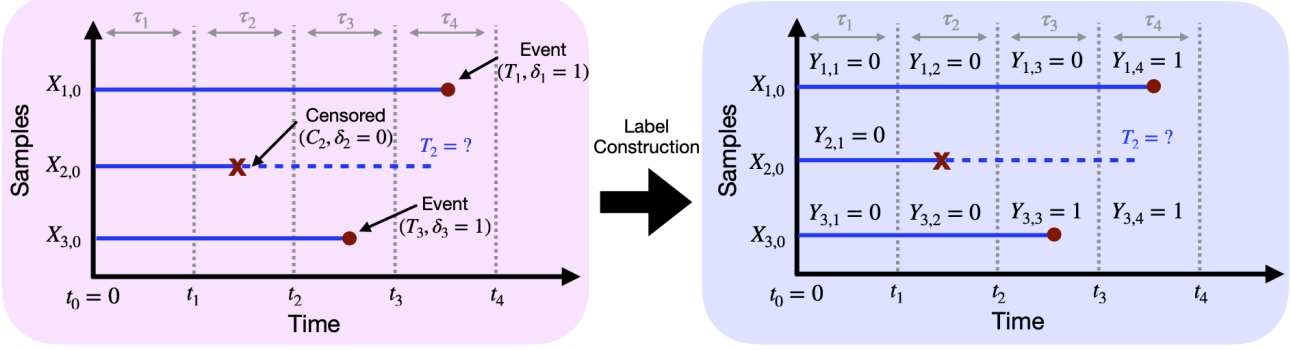


Figure 1. Transforming of survival data into a binary classification dataset (static setting). The pink panel (top left) illustrates the original time-to-event data $(X_{i,0}, T_i, C_i, \delta_i)$, where event times T_i and censoring times C_i are continuous. For second example, the event remains latent ($T_2 = ?$) after the censoring time C_2 . The blue panel (top right) displays the discretization of time into 5 intervals $\{\tau_k\}_{k=1}^5$, where binary labels $Y_{i,k} = \mathbb{1}(T_i \leq \tau_k)$ are defined at each timestep t_k for $k = 1, 2, 3, 4$. The table (bottom) shows the resulting classification dataset: each patient is transformed into at most 4 tuples, where labels are only constructed for time steps preceding the censoring time ($t_k < C_i$), highlighting the impact of right-censoring on the training set.

Practically, for training these classifiers across different history lengths (\mathcal{H}_{i,t_k} for different values of k), we featurize the inputs into a fixed dimension d vector $\phi_k(\mathcal{H}_{i,t_k}, Y_{i,1:k}, t_k, t_{k+\Delta}) \in \mathbb{R}^d$ for a vector-valued functions ϕ_k . For our classification models, we use vectors $\phi(\mathcal{H}_{i,t_k}, Y_{i,1:k}, t_k, t_{k+\Delta})$ as input and $Y_{i,t_{k+\Delta}}$ as the label. See Appendix C.2.1 for details on how we choose ϕ_k .

Inference. Given a classifier \hat{p} we estimate the dynamic survival probability $S(t_{k+\Delta} \mid T_i > t_k, \mathcal{H}_{i,t_k})$ as follows:

$$\hat{S}(t_{k+\Delta} \mid T_i > t_k, \mathcal{H}_{i,t_k}) \triangleq 1 - \hat{p}(\mathcal{H}_{i,t_k}, Y_{i,1:k}, t_k, t_{k+\Delta}). \quad (9)$$

Similar to the static setting, we clip the survival probabilities to ensure that they are monotonically decreasing in $t_{k+\Delta}$ (see Appendix C.2.1).

3.3. Theory: Consistent survival models via loss minimization

We now show formally that minimizing the losses from (5) and (8) for the static and dynamic settings, respectively, yields consistent survival models as the number of training samples increases ($n \rightarrow \infty$). This means that despite the presence of censoring, perfect binary classifiers necessarily recover the true underlying survival probabilities.

Static setting. Given infinite training data ($n \rightarrow \infty$), the

empirical loss from (5) equals the following population loss:

$$\ell_{\text{static}}(p) \triangleq \mathbb{E} \left[\sum_{k=1}^K \mathbb{1}(C_i > t_k) \cdot \text{BCE}(p(X_{i,0}, t_k), Y_{i,k}) \right]. \quad (10)$$

In Theorem 3.1 below, we show that a binary classifier p minimizes the loss $\ell(p)$ if and only if it accurately models the ground-truth survival probabilities.

Theorem 3.1 (Consistent static survival model via loss minimization). *Let p be any binary prediction model for $Y_{i,k}$ given $(X_{i,0}, t_k)$. Under Assumption 2.1 (Conditionally Independent Censoring), the population loss $\ell_{\text{static}}(p)$ is minimized if and only if, for each $k \in \{1, \dots, K-1\}$,*

$$\begin{aligned} p(x, t_k) &= \mathbb{P}(Y_{i,k} = 1 \mid X_{i,0} = x) \\ &= 1 - \mathbb{P}(T_i > t_k \mid X_{i,0} = x) \end{aligned}$$

for all x in the support of $X_{i,0}$ satisfying the positivity condition $\mathbb{P}(C_i \geq t_k \mid X_{i,0} = x) > 0$.

The equality $\mathbb{P}(Y_{i,k} = 1 \mid X_{i,0}) = 1 - \mathbb{P}(T_i > t_k \mid X_{i,0})$ above holds by the definition $Y_{i,k} \triangleq \mathbb{1}(T_i \leq t_k)$. See Appendix A.1 for the proof of Theorem 3.1.

The significance of Theorem 3.1 is that under censoring Assumption 2.1, we can perfectly learn the true survival probabilities $\mathbb{P}(T_i > t_k \mid X_{i,0})$ via loss minimization, given sufficient data. *This shows that survival analysis under temporal discretization can effectively be reduced to a supervised, binary classification problem.*

Dynamic setting. Analogously to the static setting, in the dynamic setting, we can show that as the amount of training samples grows ($n \rightarrow \infty$), minimizing the loss from (8) will necessarily lead the classifier to learn the true underlying survival probabilities. This result is very similar to Theorem 3.1; see Appendix A.2 for the statement and proof.

4. Related work

Static survival modeling. The Cox Proportional Hazards (CoxPH) model (Cox, 1972) and Random Survival Forests (Ishwaran et al., 2008) are the most established and widely utilized approaches in applied static survival analysis (Wang et al., 2019). Deep learning-based static survival models largely fall into two categories: (1) *Deep extensions of (semi-)parametric survival models* (Wiegerebe et al., 2024; Kvamme et al., 2019; Nagpal et al., 2021), e.g., DeepSurv (Katzman et al., 2018), which replaces the linear risk function in CoxPH with a neural network, and (2) *Discrete-time models* that partition the time horizon into intervals before modeling event probabilities (Lee et al., 2018; Gensheimer & Narasimhan, 2019; Chi et al., 2021); classification in survival analysis is discussed further below.

Dynamic survival modeling. The predominant dynamic survival modeling approaches fall into three categories: (1) *Landmarking*, which involves fitting a static survival model at multiple timepoints (Van Houwelingen, 2007). (2) *Deep sequence or Joint modeling*, which jointly models longitudinal observations and event times (Tsiatis & Davidian, 2004; Ibrahim et al., 2010); this includes classical statistical approaches that use linear mixed-effects models and CoxPH, as well as deep-learning variants that use recurrent neural networks with survival objectives (Giunchiglia et al., 2018; Ren et al., 2019). Recently, neural ODEs have also been used to explicitly handle irregularly sampled data (Tang et al., 2022; Moon et al., 2022). (3) *Discrete-time models*, which extend the static discrete-time models to longitudinal data (Lee et al., 2019; Kvamme & Borgan, 2021; Thorsen-Meyer et al., 2022). *Notably, the static and dynamic methods described above predominantly involve training models from scratch using specialized loss functions on a single dataset; they do not leverage pretrained representations for general-purpose survival analysis.*

Classification-based survival analysis. Multiple papers have formulated survival analysis as a classification problem. One of the first approaches was developed by Efron (1988), who used a logistic regression model to approximate the discrete hazard rate $\lambda(t_k | X_{i,0}) \triangleq \mathbb{P}(T_i \in (t_k, t_{k+1}] | X_{i,0}, T_i > t_k)$, i.e., the probability that an event occurs in the k th interval given that it has not occurred by the start of the interval. The logistic regression model is fit by maximizing the likelihood of the observed data, which factors into a function of the hazard rate; note, the likelihood of

the observed data includes both censored and uncensored examples. Singer & Willett (1993) extended this to log-odds models. This general paradigm of using binary classifiers to model the hazard rate has been termed *Survival Stacking* (Craig et al., 2025). The survival probability is recovered as the product of a function of the hazard rate: $S(t_k | X_{i,0}) = \prod_{j=1}^{k-1} \{1 - \lambda(t_j | X_{i,0})\}$. In this work, instead of modeling the hazard rate, we propose to directly model the failure probability $1 - S(t_k | X_{i,0})$. We experimented with modeling the hazard rate using TFM, but we found it performed worse in practice; we hypothesize this is due to the product-based approach to form the survival probabilities causes small estimation errors in the hazard rates over time to compound, which is avoided by directly modeling the failure probability.

Recently, DeepHit and Dynamic DeepHit (Lee et al., 2018; 2019) learn survival probabilities by training a neural network to predict which of K time intervals an event occurs in; their objective includes a ranking loss and incorporates information from censored examples. We compare against both versions in our simulations but find they significantly underperform our TFM-based approach. We hypothesize this is because DeepHit and Dynamic DeepHit require training recurrent neural networks from scratch, which is less data efficient; these models were originally evaluated on larger datasets (800-10,000 samples), while the datasets we evaluate on are much smaller (median size of ≈ 500).

5. Experimental results

Datasets. For evaluation, we use datasets from *SurvSet*, a collection of real-world, right-censored time-to-event datasets (Drysdale, 2022). These datasets span multiple domains, for example, clinical studies in biomedical research, labor datasets related to unemployment duration, as well as engineering reliability datasets concerning time to system or component failure. Out of the total 69 static and 8 dynamic datasets in *SurvSet*, we utilize 43 static and 5 dynamic datasets. We excluded datasets that (i) contained fewer than two unique event times in the test set, or (ii) had a Kaplan-Meier estimate of the censoring probability $\mathbb{P}(C_i > t_k | X_{i,0}) = 0$ or $\mathbb{P}(C_i > t_{k+\Delta} | T_i > t_k, \mathcal{H}_{i,t_k}) = 0$ for any t_k . This second criterion ensures a positive probability of not being censored; without it, the survival distribution is non-identifiable in regions lacking support, and the inverse weighting used in standard evaluation metrics leads to unstable, biased estimates (Uno et al., 2011).

Across the 43 static datasets, the median sample size is 461 (IQR: 228-1,494). The dimension of covariates $X_{i,0}$ ranged from 4 to 161 (median: 8, mean: 15.2). The censoring in these datasets is nontrivial and heterogeneous: the censoring rate ranged from 6.6% to 94.4% (median of 56.4%). The dynamic datasets vary in scale, from the 4,603 unique ex-

amples in *oldmort* to smaller ones containing between 103 and 556 samples. Across these 5 datasets, the number of covariates ranges from 4 to 7, and the censoring rate range is 27.2%-66.2%. See Appendix D.1 for more on the datasets.

5.1. Evaluation metrics

We evaluate the survival models using standard metrics for discrimination and calibration. Specifically, we assess the ability to rank-order survival times using the (time-dependent) *C-index* and the *Integrated AUC*. To quantify calibration and overall predictive accuracy, we use the *Integrated Brier Score*. **We now discuss these metrics in the static setting; we discuss dynamic analogues, specific estimators, and implementation details in Appendix B.** To ensure consistency under conditionally independent censoring (Assumption 2.1), we use Inverse-Probability-of-Censoring Weighted (IPCW) estimators for all three metrics.

Concordance index (C-Index). The C-Index quantifies a survival model’s discriminative ability by calculating the probability that, for a randomly selected pair of observations, the model assigns a higher risk to the observation that experiences the event first (Harrell et al., 1982; Uno et al., 2011). A higher C-index indicates greater discriminative ability. In the static setting, this is given by

$$C_{\text{Index}} \triangleq \mathbb{P}(\hat{r}(X_{i,0}) > \hat{r}(X_{j,0}) \mid T_i < T_j), \quad (11)$$

where \hat{r} is a risk scoring model (higher values imply earlier predicted events). For our classification-based survival models, we construct the risk score as follows:

$$\hat{r}(x) = \frac{1}{K-1} \sum_{k=1}^{K-1} \left\{ 1 - \hat{S}(t_k \mid x) \right\}. \quad (12)$$

Above, the risk score $\hat{r}(x)$ can be interpreted as the average probability that an event has occurred across all time steps t_1, \dots, t_{K-1} . This aggregate measure ensures that observations with consistently lower survival curves are assigned higher risk, even if their survival at a single specific time point is similar. For our baseline models, we discuss how we construct risk scores in Appendix C.

Integrated AUC. The time-dependent AUC assesses a model’s ability to differentiate between examples that survive up to some time t versus those that do not. In the static setting, the time-dependent AUC (Hung & Chiang, 2010) is

$$\text{AUC}(t) \triangleq \mathbb{P}(\hat{r}(X_{i,0}) > \hat{r}(X_{j,0}) \mid T_i \leq t, T_j > t), \quad (13)$$

where \hat{r} is a risk scoring model. See (12) for the risk score we use for our classification-based survival models. The Integrated AUC takes a weighted average of $\text{AUC}(t)$ over time. Specifically, in the static setting we use

$$\overline{\text{AUC}} \triangleq \frac{\sum_{k=1}^{K-1} \text{AUC}(t_k) w_{t_k}}{\sum_{k=1}^{K-1} w_{t_k}},$$

where $w_{t_k} \triangleq S(t_{k-1}) - S(t_k)$ for $S(t_k) \triangleq \mathbb{P}(T_i > t_k)$ is the marginal survival probability (Antolini et al., 2005; Lambert & Chevret, 2016). This weights the AUC by the proportion of events occurring in each interval, ensuring that the summary score reflects the model’s performance when the data is most informative and relevant.

Integrated Brier Score (IBS). The Brier Score is a mean-squared error of the estimated survival probability at time t and the true event indicator at time t (Graf et al., 1999; Kvamme & Borgan, 2023):

$$\text{BS}(t) \triangleq \mathbb{E} \left[\{ \mathbb{1}(T_i > t) - \hat{S}(t \mid X_{i,0}) \}^2 \right]. \quad (14)$$

Low Brier Scores imply the model’s survival probabilities are accurate and well-calibrated (in contrast to C-index and Integrated AUC, which only assess accurate ranking). The Integrated Brier Score averages the $\text{BS}(t)$ over time:

$$\overline{\text{BS}} \triangleq \frac{1}{t_{K-1} - t_1} \int_{t_1}^{t_{K-1}} \text{BS}(t) dt.$$

5.2. Models

Classification-based models. In both the static and dynamic settings, we use our classification-based survival modeling approach with two tabular foundation models: MITRA (Zhang et al., 2025) and TabPFN-2.5 (Grinsztajn et al., 2025). Additionally, we also include an XGBoost-based binary classifier fit on the training set as a comparison.

Static baseline models. We compare our approach to classical survival models CoxPH (Cox, 1972) and Random Survival Forest (Ishwaran et al., 2008), as well as neural survival methods DeepSurv (Katzman et al., 2018), a neural-network extension of the CoxPH model, and DeepHit (Lee et al., 2018), a temporally discretized survival model.

Dynamic baseline models. We use landmarked versions of the CoxPH and Random Survival Forest Models (Van Houwelingen, 2007). Also, we compare to two popular fully dynamic survival models: Dynamic DeepHit (Lee et al., 2019), a temporally discretized neural network based survival model, and Joint Modeling (Ibrahim et al., 2010), which simultaneously models the longitudinal trajectory of time-varying covariates with a linear mixed-effects model and the time-to-event process with a CoxPH model.

5.3. Static results

Aggregate performance trends (Table 1). Our evaluation across 43 datasets demonstrates that classification-based survival models consistently outperform existing baselines. The strong performance of XGBoost highlights the benefits of our classification formulation, while MITRA having the best overall performance demonstrates the advantage of leveraging prior knowledge in TFM. Furthermore, note

Table 1. Average performance comparison in the static setting. Our classification-based survival models, especially MITRA and XGBoost, outperform classical and neural survival baselines across all metrics on average. *Values* represent means and standard errors over 43 datasets and 5 time-discretization granularities ($K \in \{4, 5, 10, 15, 20\}$). We use *Rank* and *ELO* to characterize the head-to-head performance of the models; the best and second-best performers are highlighted in blue and orange, respectively.

Model	C-Index			Integrated AUC			Integrated Brier Score			Avg Rank ↓	Avg ELO ↑
	Value ↑	Rank ↓	ELO ↑	Value ↑	Rank ↓	ELO ↑	Value ↓	Rank ↓	ELO ↑		
MITRA	0.677 (0.016)	2.9 (0.2)	1033	0.729 (0.016)	2.7 (0.2)	1038	0.166 (0.007)	2.7 (0.2)	1037	2.8 (0.2)	1036
TabPFN	0.638 (0.020)	4.7 (0.3)	981	0.696 (0.016)	4.6 (0.3)	983	0.179 (0.008)	4.5 (0.3)	986	4.6 (0.2)	983
XGBoost	0.686 (0.017)	3.0 (0.3)	1029	0.724 (0.017)	3.0 (0.2)	1030	0.167 (0.008)	2.8 (0.2)	1034	2.9 (0.2)	1031
CoxPH	0.682 (0.017)	2.9 (0.3)	1029	0.720 (0.016)	2.9 (0.3)	1029	0.171 (0.008)	3.3 (0.3)	1019	3.1 (0.3)	1026
RSF	0.666 (0.021)	3.8 (0.3)	1007	0.716 (0.016)	3.8 (0.3)	1004	0.168 (0.007)	3.6 (0.2)	1013	3.7 (0.2)	1008
DeepHit	0.574 (0.013)	6.5 (0.2)	929	0.595 (0.015)	6.4 (0.2)	930	0.213 (0.008)	6.4 (0.2)	931	6.4 (0.2)	930
DeepSurv	0.648 (0.018)	4.3 (0.2)	992	0.686 (0.016)	4.5 (0.2)	986	0.180 (0.008)	4.8 (0.2)	979	4.5 (0.2)	986

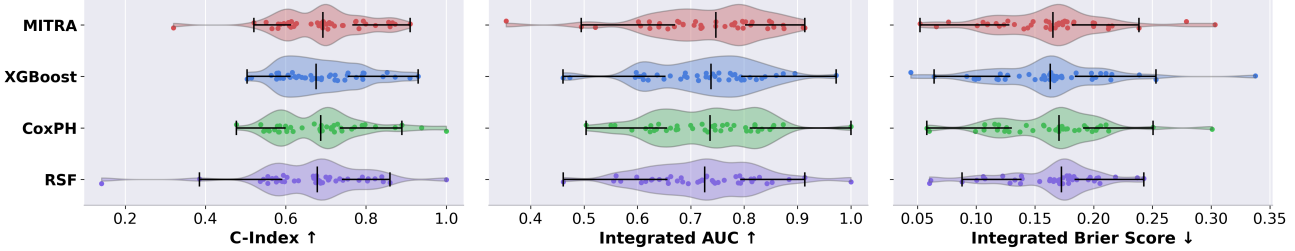


Figure 2. Performance heterogeneity in the static setting. Distribution of C-index, Integrated AUC, and IBS for the top four models across the 43 static datasets. Individual points represent specific datasets, while violin plots and vertical bars indicate the density, median, and interquartile range. Results are shown for $K = 5$ discretization bins. MITRA and XGBoost exhibit the highest median performance across all metrics. Notably, MITRA maintains the best (or close to the best) lower-performing quartile, 25th percentile for C-index/Integrated AUC and 75th percentile for IBS, compared to all other evaluated models.

that our results for all models are averaged over five different time discretization granularities $K \in \{4, 5, 10, 15, 20\}$, which highlights the strength of TFMIs is relatively robust to the choice of K . Additionally, CoxPH outperforms both DeepHit and DeepSurv, likely because deep survival models trained from scratch struggle in the small-sample regimes. These results suggest that reformulating survival as classification allows general-purpose foundation models to leverage their inductive biases more effectively.

Distribution of model performance (Figure 2). While Table 1 reports results averaged across datasets and multiple discretization scales (K), Figure 2 illustrates the performance distribution across the 43 datasets for the $K = 5$ setting. These distributions show that MITRA and XGBoost maintain better median performance across all three metrics compared to the two strongest baselines. Additionally, MITRA has the best lower-performing quartile of all the models across all metrics; specifically, its 25th percentile for C-index and Integrated AUC are comparable to or greater than those of all other models, and its 75th percentile for IBS is less than those of all other models.

Correlation between classification and survival metrics (Figure 3). We examine the relationship between *classification metrics* (binary cross-entropy loss and ROC-AUC) and *survival metrics* (C-Index and IBS) across the 43 static datasets. The moderate correlation between classification metrics and C-Index highlights that our binary objective

does not explicitly optimize for ranking. In contrast, the strong correlation ($r = 0.89$) between binary cross-entropy loss and Integrated Brier score supports our result that minimizing the binary cross-entropy loss leads to learning accurate survival probabilities (Theorem 3.1).

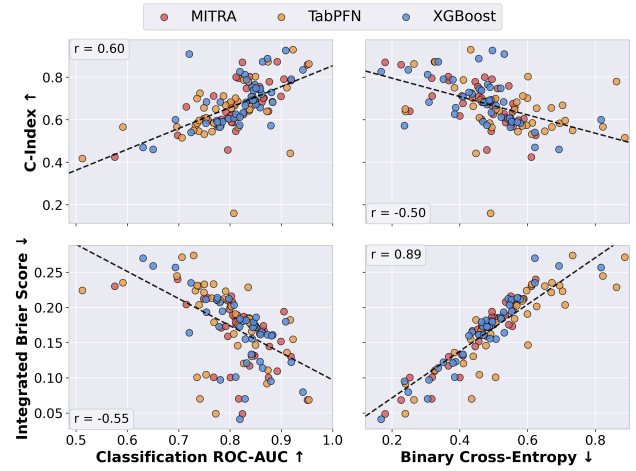


Figure 3. Correlation between classification and survival metrics (static). Each point represents a classification model evaluated on 1 of the 43 datasets. Results are shown for the test set and averaged over time-discretization granularities $K \in \{4, 5, 10, 15, 20\}$. We observe a strong correlation ($r = 0.89$) between the binary cross entropy loss and the integrated Brier score. This empirically supports our Theorem 3.1 that a model that perfectly minimizes the loss necessarily means recovers the true survival probabilities.

Table 2. Average performance comparison in the dynamic setting. Results are aggregated across 5 dynamic datasets and 3 prediction times (t_1, t_2, t_3) using $K = 5$ discretization bins. MITRA achieves the best overall performance, leading in average rank and ELO, as well as raw values for all three metrics. MITRA dominates on all metrics and Joint Model is the second best model overall. *Values* represent means and standard errors across the 5 datasets; the best and second-best performers are highlighted in blue and orange.

Model	C-Index			Integrated AUC			Integrated Brier Score			Avg Rank ↓	Avg ELO ↑
	Value ↑	Rank ↓	ELO ↑	Value ↑	Rank ↓	ELO ↑	Value ↓	Rank ↓	ELO ↑		
MITRA	0.650 (0.043)	3.8 (0.8)	1005	0.693 (0.022)	2.2 (0.2)	1053	0.099 (0.018)	1.8 (0.6)	1064	2.6 (0.2)	1041
TabPFN	0.567 (0.082)	4.0 (1.3)	999	0.632 (0.048)	4.4 (1.2)	988	0.121 (0.020)	4.8 (0.6)	976	4.4 (0.9)	988
XGBoost	0.532 (0.047)	4.8 (0.7)	977	0.600 (0.042)	4.6 (1.0)	983	0.123 (0.023)	4.6 (0.7)	982	4.7 (0.7)	981
Landmark Cox	0.615 (0.027)	3.8 (1.2)	1006	0.611 (0.077)	3.6 (1.2)	1010	0.130 (0.031)	3.8 (1.1)	1005	3.7 (1.0)	1007
Landmark RSF	0.603 (0.032)	4.0 (1.1)	1000	0.605 (0.066)	4.0 (0.5)	1000	0.104 (0.020)	3.0 (0.3)	1028	3.7 (0.6)	1009
Dynamic DeepHit	0.590 (0.032)	4.2 (0.7)	995	0.544 (0.053)	5.6 (0.2)	954	0.219 (0.026)	6.8 (0.2)	920	5.5 (0.2)	956
Joint Model	0.647 (0.051)	3.4 (1.0)	1018	0.642 (0.041)	3.6 (1.0)	1012	0.111 (0.021)	3.2 (0.8)	1024	3.4 (0.8)	1018

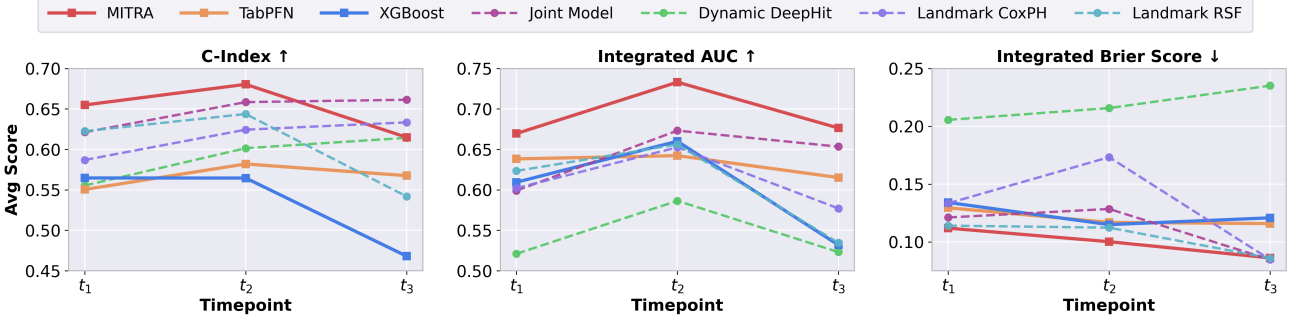


Figure 4. Performance over time in the dynamic setting. Timepoint-wise performance across the five longitudinal datasets at timepoints t_1, t_2, t_3 ($K = 5$ discretization bins). MITRA consistently outperforms both traditional landmarking baselines, joint modeling, and dynamic neural network-based survival models across most timepoints for all metrics. Notably, MITRA achieves a great lead over all other models on all three metrics at t_2 . Baseline models are represented by dashed lines.

5.4. Dynamic results

Aggregate performance trends (Table 2). In the dynamic setting, the tabular foundation model, MITRA is the best overall; specifically, it is the best on Integrated AUC and IBS, and achieves the highest average C-Index, though the Joint Model narrowly leads in C-Index rank (3.4 vs 3.8) and ELO (1018 vs. 1005). While the Joint Model has historically been a competitive method for dynamic modeling, MITRA achieves the best raw values in all metrics, most notably in Integrated AUC, outperforming the runner-up by 8% (0.693 vs. 0.642). Additionally, MITRA’s superior IBS suggests that it captures complex temporal patterns more effectively than Joint Models, which model the relationship between longitudinal inputs and risk using a specific pre-specified functional form.

The performance gap between MITRA and XGBoost widens in the dynamic setting. While XGBoost is competitive in the static setting, its significant decline in rank compared to MITRA (4.7 vs. 2.5) suggests that the temporal prior knowledge embedded in the TFM is particularly well-suited to modeling the complexities of longitudinal data. These results suggest our classification-based TFM is an effective framework for dynamic survival analysis.

Model performance over time (Figure 4). The timepoint-wise trends in Figure 4 show that MITRA’s performance

lead is most pronounced at t_2 , across all three metrics. In C-Index, MITRA has the best performance at t_1 and t_2 , but it is surpassed by the Joint Model and Landmark CoxPH at t_3 . MITRA consistently has superior performance in Integrated AUC over time, and is better than or highly competitive in IBS, particularly when the other neural model, Dynamic DeepHit, struggles.

6. Discussion

In this work, we demonstrate the utility of a classification-based formulation of survival analysis, specifically as it allows us to leverage pretrained TFM. Beyond its strong modeling performance, this approach is also computationally efficient. Using a single NVIDIA Tesla A100 GPU (80GB), our static TFM experiments (over 43 datasets and 5 time discretization granularities K for both MITRA and TabPFN) took ≈ 30 minutes. Similarly, the dynamic TFM experiments across 5 datasets took ≈ 5 minutes.

Directions for future work include (1) exploring fine-tuning and training TFM explicitly for survival analysis, e.g., to explicitly optimize for ranking or C-Index; (2) investigating ways to leverage TFM for continuous time survival modeling; and (3) leveraging TFM for treatment effect analysis in time-to-event outcomes, a common use case for survival analysis (Hosmer et al., 2008).

Acknowledgements

We thank Sonali Parbhoo for feedback on early versions of this work.

Impact Statement

This paper presents work whose goal is to advance the field of Machine Learning. There are many potential societal consequences of our work, none which we feel must be specifically highlighted here.

References

Aalen, O. Nonparametric inference for a family of counting processes. *The Annals of Statistics*, pp. 701–726, 1978.

Allison, P. D. Discrete-time methods for the analysis of event histories. *Sociological methodology*, 13:61–98, 1982.

Antolini, L., Boracchi, P., and Biganzoli, E. A time-dependent discrimination index for survival data. *Statistics in medicine*, 24(24):3927–3944, 2005.

Breslow, N. Covariance analysis of censored survival data. *Biometrics*, pp. 89–99, 1974.

Chen, G. H. et al. An introduction to deep survival analysis models for predicting time-to-event outcomes. *Foundations and Trends® in Machine Learning*, 17(6):921–1100, 2024.

Chi, S., Tian, Y., Wang, F., Wang, Y., Chen, M., and Li, J. Deep semisupervised multitask learning model and its interpretability for survival analysis. *IEEE journal of biomedical and health informatics*, 25(8):3185–3196, 2021.

Cox, D. R. Regression models and life-tables. *Journal of the Royal Statistical Society: Series B (Methodological)*, 34(2):187–202, 1972.

Craig, E., Zhong, C., and Tibshirani, R. A review of survival stacking: a method to cast survival regression analysis as a classification problem. *The International Journal of Biostatistics*, 2025.

Drysdale, E. Survset: An open-source time-to-event dataset repository. *arXiv preprint arXiv:2203.03094*, 2022.

Efron, B. Logistic regression, survival analysis, and the kaplan-meier curve. *Journal of the American statistical Association*, 83(402):414–425, 1988.

Gardner, J., Perdomo, J. C., and Schmidt, L. Large scale transfer learning for tabular data via language modeling. *Advances in Neural Information Processing Systems*, 37: 45155–45205, 2024.

Gensheimer, M. F. and Narasimhan, B. A scalable discrete-time survival model for neural networks. *PeerJ*, 7:e6257, 2019.

Giunchiglia, E., Nemchenko, A., and van der Schaar, M. Rnn-surv: A deep recurrent model for survival analysis. In *International conference on artificial neural networks*, pp. 23–32. Springer, 2018.

Graf, E., Schmoor, C., Sauerbrei, W., and Schumacher, M. Assessment and comparison of prognostic classification schemes for survival data. *Statistics in medicine*, 18(17–18):2529–2545, 1999.

Grinsztajn, L., Flöge, K., Key, O., Birkel, F., Jund, P., Roof, B., Jäger, B., Safaric, D., Alessi, S., Hayler, A., et al. TabPFN-2.5: Advancing the state of the art in tabular foundation models. *arXiv preprint arXiv:2511.08667*, 2025.

Han, C., Kim, D. W., Kim, S., You, S. C., Bae, S., and Yoon, D. Large-language-model-based 10-year risk prediction of cardiovascular disease: insight from the uk biobank data. *medRxiv*, pp. 2023–05, 2023.

Harrell, F. E., Calif, R. M., Pryor, D. B., Lee, K. L., and Rosati, R. A. Evaluating the yield of medical tests. *Jama*, 247(18):2543–2546, 1982.

Hollmann, N., Müller, S., Eggensperger, K., and Hutter, F. TabPFN: A transformer that solves small tabular classification problems in a second. In *The Eleventh International Conference on Learning Representations*, 2023. URL https://openreview.net/forum?id=cp5PvcI6w8_.

Hosmer, D. W., Lemeshow, S., and May, S. Applied survival analysis. *Wiley Series in Probability and Statistics*, pp. 60, 2008.

Hu, D., Liu, B., Li, X., Zhu, X., and Wu, N. Predicting lung cancer patient prognosis with large language models. *arXiv preprint arXiv:2408.07971*, 2024.

Hung, H. and Chiang, C.-T. Estimation methods for time-dependent auc models with survival data. *Canadian Journal of Statistics*, 38(1):8–26, 2010.

Ibrahim, J. G., Chu, H., and Chen, L. M. Basic concepts and methods for joint models of longitudinal and survival data. *Journal of clinical oncology*, 28(16):2796–2801, 2010.

Ishwaran, H., Kogalur, U. B., Blackstone, E. H., and Lauer, M. S. Random survival forests. *Annals of Applied Statistics*, 2008.

Jeanselme, V., Agarwal, N., and Wang, C. Review of language models for survival analysis. In *AAAI 2024 Spring Symposium on Clinical Foundation Models*, 2024.

Kalbfleisch, J. D. and Prentice, R. L. *The statistical analysis of failure time data*. John Wiley & Sons, 2002.

Kaplan, E. L. and Meier, P. Nonparametric estimation from incomplete observations. *Journal of the American statistical association*, 53(282):457–481, 1958.

Katzman, J. L., Shaham, U., Cloninger, A., Bates, J., Jiang, T., and Kluger, Y. Deepsurv: personalized treatment recommender system using a cox proportional hazards deep neural network. *BMC medical research methodology*, 18(1):24, 2018.

Klein, J. P. and Moeschberger, M. L. *Survival analysis: techniques for censored and truncated data*. Springer Science & Business Media, 2006.

Kvamme, H. and Borgan, Ø. Continuous and discrete-time survival prediction with neural networks. *Lifetime data analysis*, 27(4):710–736, 2021.

Kvamme, H. and Borgan, Ø. The brier score under administrative censoring: Problems and a solution. *Journal of Machine Learning Research*, 24(2):1–26, 2023.

Kvamme, H., Borgan, Ø., and Scheel, I. Time-to-event prediction with neural networks and cox regression. *Journal of machine learning research*, 20(129):1–30, 2019.

Lambert, J. and Chevret, S. Summary measure of discrimination in survival models based on cumulative/dynamic time-dependent roc curves. *Statistical methods in medical research*, 25(5):2088–2102, 2016.

Lee, C., Zame, W., Yoon, J., and Van Der Schaar, M. Deephit: A deep learning approach to survival analysis with competing risks. In *Proceedings of the AAAI conference on artificial intelligence*, volume 32, 2018.

Lee, C., Yoon, J., and Van Der Schaar, M. Dynamic-deephit: A deep learning approach for dynamic survival analysis with competing risks based on longitudinal data. *IEEE Transactions on Biomedical Engineering*, 67(1):122–133, 2019.

Little, R. J. and Rubin, D. B. *Statistical analysis with missing data*. John Wiley & Sons, 2019.

Maystre, L. and Russo, D. Temporally-consistent survival analysis. *Advances in Neural Information Processing Systems*, 35:10671–10683, 2022.

Moon, I., Groha, S., and Gusev, A. Survlatent ode: A neural ode based time-to-event model with competing risks for longitudinal data improves cancer-associated venous thromboembolism (vte) prediction. In *Machine Learning for Healthcare Conference*, pp. 800–827. PMLR, 2022.

Nagpal, C., Yadlowsky, S., Rostamzadeh, N., and Heller, K. Deep cox mixtures for survival regression. In *Machine Learning for Healthcare Conference*, pp. 674–708. PMLR, 2021.

Nelson, W. Theory and applications of hazard plotting for censored failure data. *Technometrics*, 14(4):945–966, 1972.

Pölsterl, S. scikit-survival: A library for time-to-event analysis built on top of scikit-learn. *Journal of Machine Learning Research*, 21(212):1–6, 2020.

Ren, K., Qin, J., Zheng, L., Yang, Z., Zhang, W., Qiu, L., and Yu, Y. Deep recurrent survival analysis. In *Proceedings of the AAAI conference on artificial intelligence*, volume 33, pp. 4798–4805, 2019.

Singer, J. D. and Willett, J. B. It’s about time: Using discrete-time survival analysis to study duration and the timing of events. *Journal of educational statistics*, 18(2):155–195, 1993.

Steinberg, E., Fries, J. A., Xu, Y., and Shah, N. MOTOR: A time-to-event foundation model for structured medical records. In *The Twelfth International Conference on Learning Representations*, 2024. URL <https://openreview.net/forum?id=Nialiwi2V6>.

Tang, W., Ma, J., Mei, Q., and Zhu, J. Soden: a scalable continuous-time survival model through ordinary differential equation networks. *J. Mach. Learn. Res.*, 23(1), January 2022. ISSN 1532-4435.

Thorsen-Meyer, H.-C., Placido, D., Kaas-Hansen, B. S., Nielsen, A. P., Lange, T., Nielsen, A. B., Toft, P., Schierbeck, J., Strøm, T., Chmura, P. J., et al. Discrete-time survival analysis in the critically ill: a deep learning approach using heterogeneous data. *NPJ digital medicine*, 5(1):142, 2022.

Tsiatis, A. A nonidentifiability aspect of the problem of competing risks. *Proceedings of the National Academy of Sciences*, 72(1):20–22, 1975.

Tsiatis, A. A. and Davidian, M. Joint modeling of longitudinal and time-to-event data: an overview. *Statistica Sinica*, pp. 809–834, 2004.

Uno, H., Cai, T., Pencina, M. J., D’Agostino, R. B., and Wei, L.-J. On the c-statistics for evaluating overall adequacy of risk prediction procedures with censored survival data. *Statistics in medicine*, 30(10):1105–1117, 2011.

Van Houwelingen, H. and Putter, H. *Dynamic prediction in clinical survival analysis*. CRC Press, 2011.

Van Houwelingen, H. C. Dynamic prediction by landmarking in event history analysis. *Scandinavian Journal of Statistics*, 34(1):70–85, 2007.

Vu, T., Tran, H. X., Li, X., Liu, L., Li, J., Du, J. T., and Le, T. D. Tabular foundation model for breast cancer prognosis using gene expression data. *medRxiv*, pp. 2025–10, 2025.

Wang, P., Li, Y., and Reddy, C. K. Machine learning for survival analysis: A survey. *ACM Computing Surveys (CSUR)*, 51(6):1–36, 2019.

Wiegrebé, S., Kopper, P., Sonabend, R., Bischl, B., and Bender, A. Deep learning for survival analysis: a review. *Artificial Intelligence Review*, 57(3):65, 2024.

Yu, C.-N., Greiner, R., Lin, H.-C., and Baracos, V. Learning patient-specific cancer survival distributions as a sequence of dependent regressors. *Advances in neural information processing systems*, 24, 2011.

Zhang, X., Maddix, D. C., Yin, J., Erickson, N., Ansari, A. F., Han, B., Zhang, S., Akoglu, L., Faloutsos, C., Mahoney, M. W., et al. Mitra: Mixed synthetic priors for enhancing tabular foundation models. *39th Conference on Neural Information Processing Systems (NeurIPS 2025)*, 2025.

A. Theoretical Results

A.1. Consistent static survival model

Theorem 3.1 (Consistent static survival model via loss minimization). *Let p be any binary prediction model for $Y_{i,k}$ given $(X_{i,0}, t_k)$. Under Assumption 2.1 (Conditionally Independent Censoring), the population loss $\ell_{\text{static}}(p)$ is minimized if and only if, for each $k \in \{1, \dots, K-1\}$,*

$$p(x, t_k) = \mathbb{P}(Y_{i,k} = 1 \mid X_{i,0} = x) = \mathbb{P}(T_i \leq t_k \mid X_{i,0} = x)$$

for all x in the support of $X_{i,0}$ satisfying the positivity condition $\mathbb{P}(C_i \geq t_k \mid X_{i,0} = x) > 0$. Note, by convention, we define $0 \log 0 \triangleq 0$ and $x \log 0 = -\infty$ for $x > 0$.

Proof. By the definition of $\ell_{\text{static}}(p)$ from (10),

$$\begin{aligned} \ell_{\text{static}}(p) &= -\mathbb{E} \left[\sum_{k=1}^{K-1} \mathbb{1}(C_i > t_k) \cdot \text{BCE}(p(X_{i,0}, t_k), Y_{i,k}) \right] \stackrel{(a)}{=} -\sum_{k=1}^{K-1} \mathbb{E} [\mathbb{1}(C_i > t_k) \cdot \text{BCE}(p(X_{i,0}, t_k), Y_{i,k})] \\ &\stackrel{(b)}{=} -\sum_{k=1}^{K-1} \mathbb{E} \left[\mathbb{E} [\mathbb{1}(C_i > t_k) \cdot \text{BCE}(p(X_{i,0}, t_k), Y_{i,k}) \mid X_{i,0}] \right] \\ &\stackrel{(c)}{=} -\sum_{k=1}^{K-1} \mathbb{E} \left[\mathbb{P}(C_i > t_k \mid X_{i,0}) \cdot \mathbb{E} [\text{BCE}(p(X_{i,0}, t_k), Y_{i,k}) \mid X_{i,0}] \right] \\ &\stackrel{(d)}{=} -\sum_{k=1}^{K-1} \mathbb{E} \left[\mathbb{P}(C_i > t_k \mid X_{i,0}) \cdot \mathbb{E} [Y_{i,k} \log p(X_{i,0}, t_k) + (1 - Y_{i,k}) \log (1 - p(X_{i,0}, t_k)) \mid X_{i,0}] \right] \\ &\stackrel{(e)}{=} -\sum_{k=1}^{K-1} \mathbb{E} \left[\mathbb{P}(C_i > t_k \mid X_{i,0}) \left\{ \mathbb{P}(Y_{i,k} = 1 \mid X_{i,0}) \log p(X_{i,0}, t_k) + \{1 - \mathbb{P}(Y_{i,k} = 1 \mid X_{i,0})\} \log (1 - p(X_{i,0}, t_k)) \right\} \right] \end{aligned} \tag{15}$$

Above, equality (a) holds by linearity of expectations. Equality (b) holds by the law of iterated expectations. Equality (c) holds because $C_i \perp\!\!\!\perp Y_{i,k} \mid X_{i,0}$ since $Y_{i,k} \triangleq \mathbb{1}_{T_{i,k} \leq t_k}$ and $C_i \perp\!\!\!\perp T_i \mid X_{i,0}$ by Assumption 2.1. Equality (d) holds by the definition of BCE from (6). Equality (e) holds because since $Y_{i,k}$ is binary, $\mathbb{E}[Y_{i,k} \mid X_{i,0}] = \mathbb{P}(Y_{i,k} = 1 \mid X_{i,0})$.

We will now use the result from (15) to prove the if and only if statement of the theorem. Note that by Lemma A.1,

$$\mathbb{P}(Y_{i,k} = 1 \mid X_{i,0} = x) = \operatorname{argmin}_{b \in (0,1)} -\mathbb{P}(Y_{i,k} = 1 \mid X_{i,0} = x) \log b - \{1 - \mathbb{P}(Y_{i,k} = 1 \mid X_{i,0} = x)\} \log (1 - b)$$

and the minimizer is unique. Thus, p is a minimizer of the loss $\ell_{\text{static}}(p)$ if and only if $p(x, t_k) = \mathbb{P}(Y_{i,k} = 1 \mid X_{i,0} = x)$ for all x in the support of $X_{i,0}$ for which $\mathbb{P}(C_i > t_k \mid X_{i,0} = x) > 0$. \square

Lemma A.1. *Fix $q \in [0, 1]$ and let $b \in [0, 1]$. The function $f(b) = -q \log b - (1 - q) \log(1 - b)$ is uniquely minimized at $b = q$.*

Proof. In the edge case that $q = 0$, $f(b)$ is minimized at $b = 0$. Also, when $q = 1$, $f(b)$ is minimized at $b = 1$. Now suppose $q \in (0, 1)$. Note that $f'(b) = -\frac{q}{b} + \frac{1-q}{1-b}$. When $f'(b) = 0$, we get that $b = q$. This must be the global minimizer of $f(b)$ because the second derivative of $f(b)$ is strictly positive: $f''(b) = \frac{q}{b^2} + \frac{1-q}{(1-b)^2} > 0$. \square

A.2. Consistent dynamic survival model

Analogously to the static setting, in the dynamic setting, we can show that as the amount of training samples $n \rightarrow \infty$, minimizing the loss from (8) will necessarily lead the classifier to learn the true underlying survival probabilities. Below, we define $\ell_{\text{dynamic}}(p)$, which is the population version of the loss from (8).

$$\ell_{\text{dynamic}}(p) \triangleq \mathbb{E} \left[\sum_{k=0}^{K-2} \sum_{\Delta=1}^{K-k-1} \mathbb{1}(t_k < T_i) \cdot \mathbb{1}(t_{k+\Delta} < C_i) \cdot \text{BCE}(p(\mathcal{H}_{i,t_k}, Y_{i,1:k}, t_{k+\Delta}), Y_{i,k+\Delta}) \right]. \tag{16}$$

Theorem A.2 formalizes how minimizing the loss $\ell_{\text{dynamic}}(p)$ is equivalent to learning the underlying survival probabilities, despite censoring, given that the dynamic censoring Assumption 2.2 holds.

Theorem A.2 (Consistent dynamic survival model via loss minimization). *Let p be any binary prediction model for $Y_{i,k+\Delta}$ given $(\mathcal{H}_{i,t_k}, Y_{i,1:k}, t_k, t_{k+\Delta})$. Under Assumption 2.2 (Dynamic Conditionally Independent Censoring), the population loss $\ell_{\text{dynamic}}(p)$ is minimized if and only if, for each $k \in \{1, \dots, K-2\}$ and $\Delta \in \{1, \dots, K-k-1\}$,*

$$p(h, y, t_k, t_{k+\Delta}) = \mathbb{P}(Y_{i,k+\Delta} = 1 \mid \mathcal{H}_{i,t_k} = h, Y_{i,1:k} = y) = 1 - \mathbb{P}(T_i > t_{k+\Delta} \mid \mathcal{H}_{i,t_k} = h, Y_{i,1:k} = y)$$

for all $h, y_{1:k}$ in the support of $\mathcal{H}_{i,t_k}, Y_{i,1:k}$ that (i) satisfy the positivity condition $\mathbb{P}(C_i \geq t_{k+\Delta} \mid \mathcal{H}_{i,t_k} = h, Y_{i,1:k} = y) > 0$ and (ii) have not had the event occur by t_k , i.e., $y_1 = \dots = y_k = 0$. Note, by convention, we define $0 \log 0 \triangleq 0$ and $x \log 0 = -\infty$ for $x > 0$.

Proof. By the definition of $\ell_{\text{dynamic}}(p)$ from (16),

$$\begin{aligned} \ell_{\text{dynamic}}(p) &= -\mathbb{E} \left[\sum_{k=0}^{K-2} \sum_{\Delta=1}^{K-k-1} \mathbb{1}(T_i > t_k) \cdot \mathbb{1}(C_i > t_{k+\Delta}) \cdot \text{BCE}(p(\mathcal{H}_{i,t_k}, Y_{i,1:k}, t_k, t_{k+\Delta}), Y_{i,k+\Delta}) \right] \\ &\stackrel{(a)}{=} -\sum_{k=0}^{K-2} \sum_{\Delta=1}^{K-k-1} \mathbb{E} \left[\mathbb{1}(T_i > t_k) \cdot \mathbb{1}(C_i > t_{k+\Delta}) \cdot \text{BCE}(p(\mathcal{H}_{i,t_k}, Y_{i,1:k}, t_k, t_{k+\Delta}), Y_{i,k+\Delta}) \mid \mathcal{H}_{i,t_k}, Y_{i,1:k} \right] \\ &\stackrel{(b)}{=} -\sum_{k=0}^{K-2} \sum_{\Delta=1}^{K-k-1} \mathbb{E} \left[\mathbb{1}(T_i > t_k) \cdot \mathbb{E} \left[\mathbb{1}(C_i > t_{k+\Delta}) \cdot \text{BCE}(p(\mathcal{H}_{i,t_k}, Y_{i,1:k}, t_k, t_{k+\Delta}), Y_{i,k+\Delta}) \mid \mathcal{H}_{i,t_k}, Y_{i,1:k} \right] \right] \\ &\stackrel{(c)}{=} -\sum_{k=0}^{K-2} \sum_{\Delta=1}^{K-k-1} \mathbb{E} \left[\mathbb{1}(T_i > t_k) \cdot \mathbb{P}(C_i > t_{k+\Delta} \mid \mathcal{H}_{i,t_k}, Y_{i,1:k}) \cdot \mathbb{E} \left[\text{BCE}(p(\mathcal{H}_{i,t_k}, Y_{i,1:k}, t_k, t_{k+\Delta}), Y_{i,k+\Delta}) \mid \mathcal{H}_{i,t_k}, Y_{i,1:k} \right] \right] \\ &\stackrel{(d)}{=} -\sum_{k=0}^{K-2} \sum_{\Delta=1}^{K-k-1} \mathbb{E} \left[\mathbb{1}(T_i > t_k) \cdot \mathbb{P}(C_i > t_{k+\Delta} \mid \mathcal{H}_{i,t_k}, Y_{i,1:k}) \right. \\ &\quad \times \mathbb{E} \left[Y_{i,k+\Delta} \log p(\mathcal{H}_{i,t_k}, Y_{i,1:k}, t_k, t_{k+\Delta}) + (1 - Y_{i,k+\Delta}) \log (1 - p(\mathcal{H}_{i,t_k}, Y_{i,1:k}, t_k, t_{k+\Delta})) \mid \mathcal{H}_{i,t_k}, Y_{i,1:k} \right] \\ &\stackrel{(e)}{=} -\sum_{k=0}^{K-2} \sum_{\Delta=1}^{K-k-1} \mathbb{E} \left[\mathbb{1}(T_i > t_k) \cdot \left\{ \mathbb{P}(C_i > t_{k+\Delta} \mid \mathcal{H}_{i,t_k}, Y_{i,1:k}) \cdot \mathbb{P}(Y_{i,k+\Delta} = 1 \mid \mathcal{H}_{i,t_k}, Y_{i,1:k}) \log p(\mathcal{H}_{i,t_k}, Y_{i,1:k}, t_k, t_{k+\Delta}) \right. \right. \\ &\quad \left. \left. + \{1 - \mathbb{P}(Y_{i,k+\Delta} = 1 \mid \mathcal{H}_{i,t_k}, Y_{i,1:k})\} \log (1 - p(\mathcal{H}_{i,t_k}, Y_{i,1:k}, t_k, t_{k+\Delta})) \mid \mathcal{H}_{i,t_k}, Y_{i,1:k} \right\} \right] \end{aligned} \tag{17}$$

Above, equality (a) holds by linearity of expectations. Equality (b) holds by the law of iterated expectations and since $\mathbb{1}(T_i > t_k)$ is known given $\mathcal{H}_{i,t_k}, Y_{i,1:k}$. Equality (c) holds because $C_i \perp\!\!\!\perp Y_{i,k+\Delta} \mid \mathcal{H}_{i,t_k}, Y_{i,1:k}$ since $Y_{i,k+\Delta} \triangleq \mathbb{1}_{T_{i,k+\Delta} \leq t_k}$ and $T_i \perp\!\!\!\perp C_i \mid (\mathcal{H}_{i,t_k}, T_i > t)$ by Assumption 2.2. Equality (d) holds because since $Y_{i,k+\Delta}$ is binary, $\mathbb{E}[Y_{i,k+\Delta} \mid \mathcal{H}_{i,t_k}, Y_{i,1:k}] = \mathbb{P}(Y_{i,k+\Delta} = 1 \mid \mathcal{H}_{i,t_k}, Y_{i,1:k})$.

We will now use the result from (17) to prove the if and only if statement of the theorem. Note that by Lemma A.1,

$$\begin{aligned} \mathbb{P}(Y_{i,k+\Delta} = 1 \mid \mathcal{H}_{i,t_k} = h, Y_{i,1:k} = y) &= \operatorname{argmin}_{b \in [0,1]} \{ \mathbb{P}(Y_{i,k+\Delta} = 1 \mid \mathcal{H}_{i,t_k} = h, Y_{i,1:k} = y) \log b \\ &\quad + \{1 - \mathbb{P}(Y_{i,k+\Delta} = 1 \mid \mathcal{H}_{i,t_k} = h, Y_{i,1:k} = y)\} \log (1 - b) \}, \end{aligned}$$

and the minimizer is unique. Thus, p is a minimizer of the loss $\ell_{\text{dynamic}}(p)$ if and only if $p(\mathcal{H}_{i,t_k} = h, Y_{i,1:k} = y, t_k, t_{k+\Delta}) = \mathbb{P}(Y_{i,k+\Delta} = 1 \mid \mathcal{H}_{i,t_k} = h, Y_{i,1:k} = y)$ if and only if for all h, y in the support of $\mathcal{H}_{i,t_k}, Y_{i,1:k}$ for which $\mathbb{P}(C_i > t_k \mid \mathcal{H}_{i,t_k} = h, Y_{i,1:k} = y) > 0$ and for which the event has not occurred by t_k , i.e., $y_1 = \dots = y_k = 0$. \square

B. Metrics

This appendix provides formal definitions, corresponding estimators and implementation details for the evaluation metrics used in the *static setting* and *dynamic setting*. All survival metrics are implemented using the `sksurv` library (Pösterl, 2020). We also briefly explain how we calculate the ELO rating in Section B.3. See our codebase for additional details.

B.1. Static Metrics

B.1.1. CONCORDANCE INDEX (C-INDEX)

The concordance index (C-Index) is a measure of a model's ability to accurately rank individuals by their risk of experiencing an event (Harrell et al., 1982; Uno et al., 2011). We say a pair of samples is concordant if the individual with a shorter time-to-event has a higher risk score assigned by a model.

Recall from Eq. (11), the C-Index measures the following in the static setting

$$C_{\text{Index}} \triangleq \mathbb{P}(\hat{r}(X_{i,0}) > \hat{r}(X_{j,0}) \mid T_i < T_j). \quad (18)$$

where \hat{r} is a risk scoring model. A common approach to correct for censoring is by using Inverse-Probability-of-Censoring-Weights (IPCW), which provides an unbiased and consistent estimator, under certain assumptions, including Assumption 2.1 (Uno et al., 2011). We first consider a truncated version of Eq. (18):

$$C_{\text{Index}} \triangleq \mathbb{P}(\hat{r}(X_{i,0}) > \hat{r}(X_{j,0}) \mid T_i < T_j, T_i \leq T_{\max}), \quad (19)$$

where we set T_{\max} to be the maximum observed timepoint in the train set. Truncation is used to ensure that the predicted probability of not being censored remains positive, which is required when using IPCW weighting. Following Uno et al. (2011), an IPCW estimator of Eq. (19) is

$$\hat{C}_{\text{Index}} = \frac{\sum_{i \neq j} \hat{G}(T_i)^{-2} \delta_i \mathbb{1}(T_i < T_j, T_i \leq T_{\max}) \mathbb{1}(\hat{r}(X_{i,0}) > \hat{r}(X_{j,0}))}{\sum_{i \neq j} \delta_i \hat{G}(T_i)^{-2} \mathbb{1}(T_i < T_j, T_i \leq T_{\max})},$$

where $G(t)$ denotes the population censoring function at time t . Formally,

$$G(t) \triangleq \mathbb{P}(C_i > t), \quad (20)$$

and $\hat{G}(t)$ is estimated using the Kaplan-Meier estimator (Kaplan & Meier, 1958; Pösterl, 2020).

B.1.2. INTEGRATED AUC

The AUC (area under the ROC curve) at time t is a measure of how well a model can distinguish individuals who experience an event by time t from those who do not. The weighted mean of these AUCs tells us about the overall discriminative ability of a survival model.

Recall from Eq. (13), the time-dependent AUC measures the following in the static setting

$$\text{AUC}(t) \triangleq \mathbb{P}(\hat{r}(X_{i,0}) > \hat{r}(X_{j,0}) \mid T_i \leq t, T_j > t). \quad (21)$$

A consistent IPCW estimate (Hung & Chiang, 2010) of Eq. (21) is given by

$$\widehat{\text{AUC}}(t) = \frac{\sum_{i \neq j} \hat{G}(T_i)^{-1} \delta_i \mathbb{1}(T_i \leq t, T_j > t) \mathbb{1}(\hat{r}(X_{i,0}) > \hat{r}(X_{j,0}))}{\sum_{i \neq j} \hat{G}(T_i)^{-1} \delta_i \mathbb{1}(T_i \leq t, T_j > t)}, \quad (22)$$

where $G(t)$ is the censoring function at time t ; see Eq. (20). We evaluate Eq. (22) at t_k for $k \in \{1, \dots, K-1\}$, and compute a weighted average of the resulting AUCs, using the estimated survival function as weights

$$\overline{\text{AUC}} = \frac{\sum_{k'=1}^{K-1} \widehat{\text{AUC}}(t_{k'}) w_{t_{k'}}}{\sum_{k'=1}^{K-1} w_{t_{k'}}},$$

where $w_{t_k} = \hat{S}(t_{k-1}) - \hat{S}(t_k)$, and $\hat{S}(t)$ is the Kaplan-Meier estimator of the marginal survival function: $S(t) \triangleq \mathbb{P}(T_i > t)$ (Kaplan & Meier, 1958).

B.1.3. INTEGRATED BRIER SCORE (IBS)

The Integrated Brier Score quantifies a model's calibration and accuracy by averaging over time, the squared error between the predicted survival probabilities and the observed survival outcomes. Recall from Eq. (14), the time-dependent Brier score at time t is defined as the mean squared error between the binary outcome $\mathbb{1}(T_i > t)$ and the predicted survival function

$$\text{BS}(t) \triangleq \mathbb{E}\left[\left(\mathbb{1}(T_i > t) - \hat{S}(t | X_{i,0})\right)^2\right]. \quad (23)$$

A standard IPCW estimator of Eq. (23) from Kvamme & Borgan (2023) is

$$\widehat{\text{BS}}(t) = \frac{1}{n} \sum_{i=1}^n \left[\frac{\mathbb{1}(T_i \leq t, \delta_i = 1)}{\hat{G}(T_i)} (0 - \hat{S}(t | X_{i,0}))^2 + \frac{\mathbb{1}(T_i > t)}{\hat{G}(t)} (1 - \hat{S}(t | X_{i,0}))^2 \right], \quad (24)$$

where $G(t)$ is the censoring function at time t , defined in Eq. (20). We estimate the Integrated Brier Score by evaluating Eq. (24) at time points t_k , $k \in \{1, \dots, K-1\}$, and then integrating these values over time

$$\overline{\text{BS}} = \frac{1}{t_{K-1} - t_1} \int_{t_1}^{t_{K-1}} \widehat{\text{BS}}(t) dt.$$

We use the trapezoidal rule to approximate the integral.

B.2. Dynamic Metrics

Risk scores. A risk score is a real-valued prediction of an individual's risk, where higher values correspond to a greater risk of experiencing the event. We denote the risk scoring model by \hat{r} . In the static setting, $\hat{r}(X_{i,0})$ denotes a risk score for individual i given baseline covariates $X_{i,0}$. In the dynamic setting, $\hat{r}(\mathcal{H}_{i,t_k})$ denotes the time-dependent risk score for individual i at time t_k , computed using the history available up to time t_k .

B.2.1. CONCORDANCE INDEX (C-INDEX)

In the dynamic setting, the C-Index at time t is defined as

$$C_{\text{Index}}(t) \triangleq \mathbb{P}(\hat{r}(\mathcal{H}_{i,t}) > \hat{r}(\mathcal{H}_{j,t}) \mid t < T_i < T_j), \quad (25)$$

where the risk scores are computed using history available up to t . Analogous to the static setting (see Appendix B.1.1), we can define a truncated, IPCW estimator of Eq. (25)

$$\hat{C}_{\text{Index}}(t) = \frac{\sum_{i \neq j} \hat{G}(T_i \mid t)^{-2} \delta_i \mathbb{1}(t < T_i < T_j, T_i \leq T_{\max}) \mathbb{1}(\hat{r}(\mathcal{H}_{i,t}) > \hat{r}(\mathcal{H}_{j,t}))}{\sum_{i \neq j} \delta_i \hat{G}(T_i \mid t)^{-2} \mathbb{1}(t < T_i < T_j, T_i \leq T_{\max})},$$

where $G(t + \Delta \mid t)$ denotes the conditional censoring function, or formally

$$G(t + \Delta \mid t) \triangleq \mathbb{P}(C_i > t + \Delta \mid C_i > t), \quad (26)$$

which is the probability of remaining uncensored up to time $t + \Delta$ given being uncensored at time t . Similar to the static setting, $\hat{G}(t + \Delta \mid t)$ is estimated using the Kaplan-Meier estimator (Kaplan & Meier, 1958; Pöhlsterl, 2020).

B.2.2. INTEGRATED AUC

In the dynamic setting, the time dependent AUC at time $t + \Delta$, given survival up to t is given by

$$\text{AUC}(t + \Delta \mid t) \triangleq \mathbb{P}(\hat{r}(\mathcal{H}_{i,t}) > \hat{r}(\mathcal{H}_{j,t}) \mid t < T_i \leq t + \Delta < T_j) \quad (27)$$

Analogous to the static setting (see Appendix B.1.2), we form the following IPCW estimate of Eq. (27)

$$\widehat{\text{AUC}}(t + \Delta \mid t) = \frac{\sum_{i \neq j} \hat{G}(T_i \mid t)^{-1} \delta_i \mathbb{1}(t < T_i \leq t + \Delta < T_j) \mathbb{1}(\hat{r}(\mathcal{H}_{i,t}) > \hat{r}(\mathcal{H}_{j,t}))}{\sum_{i \neq j} \hat{G}(T_i \mid t)^{-1} \delta_i \mathbb{1}(t < T_i \leq t + \Delta < T_j)},$$

where $G(t + \Delta \mid t)$ is the conditional censoring function; see Eq. (26).

At each conditioning time t_k , we select the future evaluation timepoints $t_{k+\Delta}$ from the discretized horizons. For example, if the time grid is t_1, \dots, t_4 and we condition on survival up to t_2 , we compute the time dependent AUC for $\text{AUC}(t_3 \mid t_2)$ and $\text{AUC}(t_4 \mid t_2)$, which assess the accuracy of the predicted survival probabilities at times t_3 and t_4 given information available up to t_2 .

Under our discretized setting, we estimate the Integrated AUC at t_k by

$$\overline{\text{AUC}}(t_k) = \frac{\sum_{\Delta=1}^{K-k-1} \widehat{\text{AUC}}(t_{k+\Delta} \mid t_k) w_{t_{k+\Delta}}}{\sum_{\Delta=1}^{K-k-1} w_{t_{k+\Delta}}},$$

where $w_{t_{k+\Delta}} = \hat{S}(t_{k+\Delta-1} \mid t_k) - \hat{S}(t_{k+\Delta} \mid t_k)$, and $\hat{S}(t + \Delta \mid t)$ is the Kaplan–Meier estimator of the population survival function at $t + \Delta$, given survival up to t , i.e. $S(t + \Delta \mid t) \triangleq \mathbb{P}(T_i > t + \Delta \mid T_i > t)$.

B.2.3. INTEGRATED BRIER SCORE (IBS)

In the dynamic setting, the time dependent Brier Score at time $t + \Delta$, given survival up to t can be defined as

$$\text{BS}(t + \Delta \mid t) \triangleq \mathbb{E} \left[\left(\mathbb{1}\{T_i > t + \Delta\} - \hat{S}(t + \Delta \mid T_i > t, \mathcal{H}_{i,t}) \right)^2 \right]. \quad (28)$$

An analogous estimator for Eq. (28) is

$$\begin{aligned} \widehat{\text{BS}}(t + \Delta \mid t) = \frac{1}{n} \sum_{i=1}^n \left[\frac{\mathbb{1}(t < T_i \leq t + \Delta, \delta_i = 1)}{\hat{G}(T_i \mid t)} \left(0 - \hat{S}(t + \Delta \mid T_i > t, \mathcal{H}_{i,t}) \right)^2 \right. \\ \left. + \frac{\mathbb{1}(T_i > t + \Delta)}{\hat{G}(t + \Delta \mid t)} \left(1 - \hat{S}(t + \Delta \mid T_i > t, \mathcal{H}_{i,t}) \right)^2 \right], \end{aligned}$$

where $G(t + \Delta \mid t)$ is the conditional censoring function, as in Eq. (26).

Similar to the dynamic Integrated AUC, for each conditioning time t_k , we select the future evaluation timepoints $t_{k+\Delta}$ from the discretized horizons. Under this discretized setting, the Integrated Brier Score at time t_k can be estimated by

$$\overline{\text{BS}}(t_k) = \frac{1}{t_{K-1} - t_{k+1}} \int_{t_{k+1}}^{t_{K-1}} \widehat{\text{BS}}(t \mid t_k) dt.$$

B.3. ELO Rating

The Elo rating system is a method for ranking competitors based on the outcomes of pairwise comparisons. Each model is assigned a numerical rating that reflects its relative performance, with higher values indicating better performance. All models start from the same initial rating (which we set to 1000), and their ratings are updated after each comparison depending on whether a model performs better or worse than expected given its current rating. We implement Elo using the `elote` Python package¹ with the default K -factor of 32, which controls how strongly each comparison influences the ratings.

Static setting. In the static setting, performance is reported for multiple values of time discretization granularities $K \in \{4, 5, 8, 10, 15, 20\}$. We first average each model’s metric values across all K values within each dataset. Using these aggregated values, we build one Elo arena per dataset and compare all models pairwise. The final static Elo score is the average of a model’s Elo ratings across datasets.

Dynamic setting. In the dynamic setting, performance is reported at multiple time points and we use a single time discretization granularity $K = 5$. We aggregate each model’s metric values over time points t_1, t_2, t_3 within each dataset. Using these time-aggregated values, we again build one Elo arena per dataset and compare all models pairwise. The final dynamic Elo score is the average of a model’s Elo ratings across datasets.

¹<https://pypi.org/project/elote/>

C. Modeling Details

C.1. Static Models

C.1.1. CLASSIFICATION-BASED MODELS

Subsampling. The context windows of tabular foundation models are generally limited. To manage this, after constructing the supervised learning dataset as described in Section 3.1, we randomly subsample the training set to the maximum number of rows supported by each model when needed (10,000 for MITRA and 50,000 for TabPFN); no such limit is imposed for XGBoost².

Clipping survival probabilities. To ensure our survival probabilities are non-increasing in time, we apply a post-processing step that enforces monotonicity over time. Specifically, we refine our definition of $\hat{S}(t_k | X_{i,0})$ from Eq. (7) as follows:

$$\hat{S}(t_k | X_{i,0}) \triangleq \min_{j \leq k} 1 - \hat{p}(X_{i,0}, t_k).$$

This ensures that $\hat{S}(t_1 | X_{i,0}) \geq \hat{S}(t_2 | X_{i,0}) \geq \dots \geq \hat{S}(t_{K-1} | X_{i,0})$. Our definition of the risk score from Eq. (12) uses these clipped survival probabilities.

C.1.2. COX PROPORTIONAL HAZARDS (COXPH)

We use the `sksurv` package to implement the CoxPH model.³ The CoxPH model relates the baseline covariates $X_{i,0}$ to the hazard of an event at time t using $\lambda(t | X_{i,0}) = \lambda_0(t) \exp((X_{i,0})^\top \beta)$, where β is the vector of regression coefficients, and $\lambda_0(t)$ is the baseline hazard function, a population-level function defined as the hazard for the baseline covariate $X = \mathbf{0}$.

$$\lambda_0(t) \triangleq \lambda(t | X_{i,0} = \mathbf{0}). \quad (29)$$

The coefficients β are estimated by maximizing the Cox partial likelihood function (Cox, 1972). Let $\hat{\beta}$ denote the fitted coefficients, the risk score for an individual i is defined as the inner product between the covariates and the coefficients:

$$\hat{r}(X_{i,0}) = X_{i,0}^\top \hat{\beta}.$$

The corresponding survival function is

$$\hat{S}(t | X_{i,0}) = \hat{S}_0(t)^{\exp(X_{i,0}^\top \hat{\beta})},$$

where $\hat{S}_0(t)$ is the estimated baseline survival function, i.e., the survival function for the reference covariate value $X_{i,0} = \mathbf{0}$. Formally, the baseline survival function is

$$S_0(t) \triangleq \mathbb{P}(T > t | X_{i,0} = \mathbf{0}), \quad (30)$$

and $\hat{S}_0(t)$ is estimated using the Breslow estimator (Breslow, 1974).

C.1.3. RANDOM SURVIVAL FORESTS (RSF)

We use the `sksurv` RSF implementation.⁴ RSF is a nonparametric ensemble model that extends random forests to right-censored survival data by learning an ensemble of tree-based cumulative hazard functions (Ishwaran et al., 2008). An RSF consists of an ensemble of B survival trees. Each tree partitions the feature space into terminal nodes, and for each terminal node a cumulative hazard function is estimated from the training samples in that node using the Nelson-Aalen estimator (Nelson, 1972; Aalen, 1978). For an individual i , let $\ell_b(X_{i,0})$ denote the terminal node in tree b to which $X_{i,0}$ is assigned. The tree-level cumulative hazard is given by $\hat{H}_b(t | X_{i,0}) = \hat{H}_{b, \ell_b(X_{i,0})}(t)$. The forest-level cumulative hazard is obtained by averaging over trees: $\hat{H}(t | X_{i,0}) = \frac{1}{B} \sum_{b=1}^B \hat{H}_b(t | X_{i,0})$. The risk score for an individual i can be computed as follows:

$$\hat{r}(X_{i,0}) = \sum_{t' \in \mathcal{T}} \hat{H}(t' | X_{i,0}),$$

²<https://pypi.org/project/xgboost/>

³https://scikit-survival.readthedocs.io/en/stable/api/generated/sksurv.linear_model.CoxPHSurvivalAnalysis.html

⁴<https://scikit-survival.readthedocs.io/en/stable/api/generated/sksurv.ensemble.RandomSurvivalForest.html>

where \mathcal{T} is a set that contains all the distinct event times observed in the training data. The corresponding survival function is computed from the forest-level cumulative hazard as

$$\hat{S}(t \mid X_{i,0}) = \exp(-\hat{H}(t \mid X_{i,0})).$$

C.1.4. DEEPSURV

We use the `pycox` implementation of DeepSurv.⁵ DeepSurv is a neural-network extension of the CoxPH model in which the linear risk function is replaced by a nonlinear function learned by a deep neural network (Katzman et al., 2018). In DeepSurv, the hazard for an individual with covariates $X_{i,0}$ is $\lambda(t \mid X_{i,0}) = \lambda_0(t) \exp(f_\theta(X_{i,0}))$, where $\lambda_0(t)$ is the baseline hazard defined in Eq. (29) and $f_\theta(X_{i,0})$ is a neural network with parameters θ that replaces the linear term $(X_{i,0})^\top \beta$ in CoxPH. The network weights θ are then learned by maximizing the Cox partial likelihood. After training, the risk score for an individual i is

$$\hat{r}(X_{i,0}) = f_\theta(X_{i,0}),$$

and the corresponding survival function is

$$\hat{S}(t \mid X_{i,0}) = \hat{S}_0(t)^{\exp(f_\theta(X_{i,0}))},$$

where $\hat{S}_0(t)$ is the estimated baseline survival function defined in Eq. (30); we use the Breslow estimator (Breslow, 1974).

C.1.5. DEEPHIT

We use the `pycox` implementation of DeepHit.⁶ DeepHit is a neural-network-based, nonparametric survival model that directly learns the discrete-time distribution of event times without assuming proportional hazards (Lee et al., 2018). We apply a discretization setting similar to our classifier-based models as described in Section 3. For an input $X_{i,0}$, the network outputs a probability mass function over a discretized time with K ordered time bins. Specifically, DeepHit produces estimates

$$p_{\theta,k}(X_{i,0}) \approx \mathbb{P}(T_i \in \tau_k \mid X_{i,0}), \quad k = 1, \dots, K,$$

where $\tau_k = (t_{k-1}, t_k]$ are time bins induced by cut points $0 = t_0 < \dots < t_K = \infty$. We obtain the risk score by computing the negative expected bin index under the predicted distribution,

$$\hat{r}(X_{i,0}) = - \sum_{k=1}^K k p_{\theta,k}(X_{i,0}).$$

The survival probability at t_k is then given by

$$\hat{S}(t_k \mid X_{i,0}) = 1 - \sum_{j=1}^k p_{\theta,j}(X_{i,0}).$$

C.2. Dynamic Models

Last-Observation-Carried-Forward (LOCF). We employ a slightly modified version of the last-observation-carried-forward (LOCF) method in several of the dynamic models to represent the information available up to a particular time (Little & Rubin, 2019). Recall from Eq. (3) that dynamic survival prediction focuses on the conditional survival probability for a future horizon $\Delta > 0$, given the information available at time t . Since the covariates are usually observed at irregular intervals, their covariate values are generally not available exactly at time t . We therefore apply the LOCF method, where the time-dependent covariate at time t is imputed by its most recent observed value prior to t .

Recall from Section 2.2 that the observed covariate history for individual i up to time t is $\mathcal{H}_{i,t} \triangleq \{(s, X_{i,s}) : s \in \mathcal{T}_i, s \leq t\}$, where \mathcal{T}_i denotes the set of observation times for individual i . Define the most recent observation time prior to t by

$$s_i(t) \triangleq \arg \max_{s \in \mathcal{T}_i: s \leq t} s.$$

The LOCF representation of the covariate history at time t is then

$$X_{i,t}^{\text{LOCF}} \triangleq X_{i,s_i(t)}. \tag{31}$$

⁵<https://github.com/havakv/pycox>

⁶<https://github.com/havakv/pycox>

C.2.1. CLASSIFICATION-BASED MODELS

Representation of history ϕ during training. Recall from Section 3.2, the classification-based dynamic models (MITRA, TabPFN, and XGBoost) take the vector-valued function $\phi_k(\mathcal{H}_{i,t_k}, Y_{i,1:k}, t_k, t_{k+\Delta})$ as input, and predict the binary label $Y_{i,t_{k+\Delta}}$ during training. Let \bar{X}_{i,t_k} be the running means of the covariates computed up to t_k . We consider the following feature representations:

- Base representation: $\phi_k(\mathcal{H}_{i,t_k}, Y_{i,1:k}, t_k, t_{k+\Delta}) = [X_{i,t_k}^{\text{LOCF}}, \bar{X}_{i,t_k}, t_k, t_{k+\Delta}]$
- Representation incorporating the time elapsed since the most recent observation prior to t_k :

$$\phi_k(\mathcal{H}_{i,t_k}, Y_{i,1:k}, t_k, t_{k+\Delta}) = [X_{i,t_k}^{\text{LOCF}}, \bar{X}_{i,t_k}, t_k, t_{k+\Delta}, t_k - s_i(t_k)]$$
- Representation incorporating the info (i.e. the index) of the prediction horizon:

$$\phi_k(\mathcal{H}_{i,t_k}, Y_{i,1:k}, t_k, t_{k+\Delta}) = [X_{i,t_k}^{\text{LOCF}}, \bar{X}_{i,t_k}, t_k, t_{k+\Delta}, k + \Delta]$$
- Full Representation:

$$\phi_k(\mathcal{H}_{i,t_k}, Y_{i,1:k}, t_k, t_{k+\Delta}) = [X_{i,t_k}^{\text{LOCF}}, \bar{X}_{i,t_k}, t_k, t_{k+\Delta}, t_k - s_i(t_k), k + \Delta]$$

See Appendix D.3 on how we select which representation to use.

Clipping Survival Probabilities. Since $\hat{S}(t_{k+\Delta} \mid T_i > t_k, \mathcal{H}_{i,t_k})$ must be non-increasing in Δ , we apply a similar monotonicity post-processing described in Appendix C.1.1. We refine Eq. (9) by the following

$$\hat{S}(t_{k+\Delta} \mid T_i > t_k, \mathcal{H}_{i,t_k}) \triangleq \min_{1 \leq \ell \leq \Delta} 1 - \hat{p}(\mathcal{H}_{i,k}, Y_{i,1:k}, t_k, t_{k+\ell}), \quad \Delta = 1, \dots, K - 1 - k.$$

This ensures that $\hat{S}(t_{k+1} \mid t_k, \mathcal{H}_{i,t_k}) \geq \hat{S}(t_{k+2} \mid t_k, \mathcal{H}_{i,t_k}) \geq \dots \geq \hat{S}(t_{K-1} \mid t_k, \mathcal{H}_{i,t_k})$.

The time-dependent risk score is defined by averaging the predicted future cumulative risks over the remaining time horizon. For individual i at time t_k , the risk score is

$$\hat{r}(\mathcal{H}_{i,t_k}) = \frac{1}{K - 1 - k} \sum_{\Delta=1}^{K-1-k} \left(1 - \hat{S}(t_{k+\Delta} \mid T_i > t_k, \mathcal{H}_{i,t_k}) \right).$$

C.2.2. LANDMARK COXPH

Since the Cox Proportional Hazards (CoxPH) model requires static covariates, we adopt the landmarking approach using LOCF (Little & Rubin, 2019). Again, we use the `sksurv` package to implement the CoxPH model. For each t_k , the covariate history is represented by

$$\phi_{\text{landmark}}(\mathcal{H}_{i,t_k}) \triangleq (X_{i,t_k}^{\text{LOCF}}, \bar{X}_{i,t_k}) \quad (32)$$

where we also included the running means of the covariates computed up to t_k , \bar{X}_{i,t_k} . For each $t_k, k \in \{1, \dots, K-2\}$, we fit a separate CoxPH model using only individuals who are still event-free at t_k . Each landmark CoxPH model yields regression coefficient estimates $\hat{\beta}_{t_k}$. Analogous to the static setting of the CoxPH model (see Appendix C.1.2), the time-dependent risk score for individual i at t_k can be computed as

$$\hat{r}(\mathcal{H}_{i,t_k}) = \phi_{\text{landmark}}(\mathcal{H}_{i,t_k})^\top \hat{\beta}_{t_k}.$$

Survival predictions over a horizon $\Delta > 0$ are obtained conditionally on survival up to t_k :

$$\hat{S}(t_{k+\Delta} \mid T_i > t_k, \mathcal{H}_{i,t_k}) = \hat{S}_0(t_{k+\Delta} \mid t_k)^{\exp(\hat{r}(\mathcal{H}_{i,t_k}))}.$$

where $\hat{S}_0(t_{k+\Delta} \mid t_k)$ is the estimated baseline survival function, i.e., the survival function for a reference individual with zero covariates. Formally, the baseline survival function conditional on time t_k is

$$S_0(t_{k+\Delta} \mid t_k) \triangleq \mathbb{P}(T > t_{k+\Delta} \mid T > t_k, \phi_{\text{landmark}}(\mathcal{H}_{i,t_k}) = 0), \quad (33)$$

and $\hat{S}_0(t_{k+\Delta} \mid t_k)$ is estimated using the Breslow estimator (Breslow, 1974).

C.2.3. LANDMARK RANDOM SURVIVAL FOREST

Similar to the landmark CoxPH model, at each landmark time t_k , $k \in \{1, \dots, K-2\}$, we fit a separate random survival forest (RSF) using only individuals who are event-free at t_k , $\phi_{\text{landmark}}(\mathcal{H}_{i,t_k})$ defined in Eq. (32) as a representation of the history. Again, we use the `sksurv` RSF implementation. Each landmark-specific forest estimates a cumulative hazard function for $t \geq t_k$, $\hat{H}_{t_k}(t \mid T_i > t_k, \mathcal{H}_{i,t_k})$. The time-dependent risk score for individual i at landmark time t_k is defined as

$$\hat{r}(\mathcal{H}_{i,t_k}) = \sum_{t' \in \mathcal{T}} \hat{H}_{t_k}(t' \mid T_i > t_k, \mathcal{H}_{i,t_k}),$$

where \mathcal{T} is a set that contains all the distinct event times observed in the training data. The corresponding survival probability over a horizon Δ , conditional on survival up to the landmark time, is given by

$$\hat{S}(t_{k+\Delta} \mid T_i > t_k, \mathcal{H}_{i,t_k}) = \exp\left(-\hat{H}_{t_k}(t_{k+\Delta} \mid T_i > t_k, \mathcal{H}_{i,t_k})\right).$$

C.2.4. DYNAMIC DEEPHIT

Dynamic DeepHit (Lee et al., 2019) extends DeepHit to the dynamic setting by modeling the conditional distribution of future event times given an individual's longitudinal history. We use the following public implementation: <https://github.com/Jeanselme/DynamicDeepHit/tree/main>

We use a fixed discretization with K time bins that aligns with the time discretization approach described in Section 3. The implementation of Dynamic DeepHit takes as input the longitudinal history \mathcal{H}_{i,t_k} and outputs the estimates of the cumulative incidence distribution,

$$\hat{p}_{t_k, k+\Delta}(\mathcal{H}_{i,t_k}) \approx \mathbb{P}(T_i \leq t_{k+\Delta} \mid T_i > t_k, \mathcal{H}_{i,t_k}), \quad \Delta = 1, \dots, K-k-1.$$

We define the time-dependent risk score at time t_k as the predicted probability of experiencing the event in the next interval,

$$\hat{r}(\mathcal{H}_{i,t_k}) = \hat{p}_{t_k, k+1}(\mathcal{H}_{i,t_k}).$$

The conditional survival probability at $t_{k+\Delta}$ given survival up to t_k is

$$\hat{S}(t_{k+\Delta} \mid T_i > t_k, \mathcal{H}_{i,t_k}) = 1 - \hat{p}_{t_k, k+\Delta}(\mathcal{H}_{i,t_k}).$$

C.2.5. JOINT MODEL

The joint model links a longitudinal process and a survival outcome through shared subject-specific random effects (Ibrahim et al., 2010). We implement the joint model using the `JMbayes2` package.⁷ We model the longitudinal process using a linear mixed-effects model, while the survival outcome is modeled using a CoxPH model.

Given survival up to a time t_k and the observed longitudinal history \mathcal{H}_{i,t_k} the joint model yields dynamic survival predictions at future times $t_{k+\Delta} > t_k$. At each t_k , the predicted event probability at a future time point $t_{k+\Delta}$ is denoted using $\hat{p}_{t_k, k+\Delta}(\mathcal{H}_{i,t_k})$, which can be obtained by calling the `predict()` function in the `JMbayes2` package. We define the time-dependent risk score at t_k as the predicted probability the event occurs at the next interval

$$\hat{r}(\mathcal{H}_{i,t_k}) = \hat{p}_{t_k, k+1}(\mathcal{H}_{i,t_k}),$$

and the conditional survival probability at $t_{k+\Delta}$ can be computed using

$$\hat{S}(t_{k+\Delta} \mid T_i > t_k, \mathcal{H}_{i,t_k}) = 1 - \hat{p}_{t_k, k+\Delta}(\mathcal{H}_{i,t_k}).$$

⁷<https://cran.r-project.org/web/packages/JMbayes2/index.html>

D. Experimental Details

D.1. Datasets

Static. Across 43 static datasets, (Drysdale, 2022) the median number of unique samples was 461 (range 26–6805). The number of covariates ranged from 3 to 160. The censoring rate ranged from 6.6% to 94.4%.

Table 3. Summary statistics for each static survival dataset.

No.	Dataset	No. of covariates	No. of unique samples	Censoring (%)
1	Aids2	4	2839	38.0
2	Dialysis	4	6805	76.4
3	Framingham	7	4699	68.7
4	GBSG2	8	686	56.4
5	Melanoma	5	205	72.2
6	TRACE	6	1878	49.0
7	UnempDur	6	3241	38.7
8	Unemployment	5	452	43.4
9	actg	11	1151	91.7
10	breast	4	100	74.0
11	burn	11	154	68.8
12	cancer	8	228	27.6
13	cgd	10	128	65.6
14	colon	9	929	51.3
15	cost	13	518	22.0
16	d.oropharec	12	192	27.6
17	dataDIVAT1	5	5943	83.6
18	dataDIVAT2	4	1837	68.3
19	dataDIVAT3	7	4267	94.4
20	dataOvarian1	160	912	40.4
21	diabetes	4	197	60.7
22	e1684	3	284	31.0
23	follic	5	541	35.7
24	glioma	4	37	37.8
25	hepatoCellular	43	227	57.3
26	mgus	9	241	6.6
27	nki70	75	144	66.7
28	nwtco	7	4028	85.8
29	ova	5	358	25.7
30	ovarian	4	26	53.8
31	pbc	6	312	59.9
32	phpl04K8a	21	442	46.6
33	prostate	15	502	29.5
34	rdata	4	1040	47.4
35	retinopathy	7	197	60.7
36	scania	5	1931	43.8
37	smarto	26	3873	88.1
38	stagec	7	146	63.0
39	uis	8	628	19.1
40	veteran	6	137	6.6
41	vlbw	22	617	82.7
42	whas500	16	461	61.8
43	zinc	13	431	81.2

Dynamic. Across 5 dynamic datasets (Drysdale, 2022), the median number of unique samples was 467 (range 103–4603). The number of covariates ranged from 4 to 7. The patient-wise censoring rate ranged from 27.2% to 66.2%.

Table 4. Summary statistics for each dynamic survival dataset.

No.	Dataset	No. of covariates	No. of unique samples	Censoring (%)
1	aids	5	467	59.7
2	csl	6	446	39.5
3	epileptic	5	556	66.2
4	heart	4	103	27.2
5	oldmort	7	4603	57.2

D.2. Data Preprocessing

We split each dataset into training, validation, and test sets (70:15:15) using a stratified procedure on the event indicator to preserve the event–censoring proportion across splits. Categorical covariates were then transformed via one-hot encoding, fitted on the training set, and the resulting feature matrices for the validation and test sets were aligned to the training design matrix by adding any missing dummy columns and filling them with zeros. Missing covariate values were handled using a `SimpleImputer`⁸ fit on the training data only and subsequently applied to the validation and test sets, ensuring that no information from the held-out splits informed preprocessing.

D.3. Hyperparameters

Model selection approach. For each dataset, we select hyperparameters using the best performing model in terms of *C-Index* (IPCW estimator) on the validation split.

Static search spaces For the baselines, we perform a small grid search:

- **CoxPH:** ℓ_2 regularization strength $\alpha \in \{10^{-6}, 10^{-3}, 10^{-1}\}$.
- **RSF:** number of trees $n_{\text{estimators}} \in \{50, 100, 200\}$, min split $\in \{2, 5, 10, 20\}$.
- **DeepSurv:** dropout $\in \{0, 0.1\}$, hidden layers $\in \{(128, 32), (256, 32), (512, 32)\}$, learning rate $\in \{10^{-3}, 10^{-4}, 10^{-5}\}$.
- **DeepHit:** dropout $\in \{0, 0.1\}$, hidden layers $\in \{(128, 32), (256, 32), (512, 32)\}$, learning rate $\in \{10^{-3}, 10^{-4}, 10^{-5}\}$.

Note that we do not define any hyperparameters for the classifier models in the static setting.

Dynamic search spaces For the baselines, we perform a small grid search:

- **Landmark CoxPH:** ℓ_2 regularization strength $\alpha \in \{10^{-6}, 10^{-3}, 10^{-1}\}$.
- **Landmark RSF:** number of trees $n_{\text{estimators}} \in \{100, 200, 500, 1000\}$, max depth $\in \{3, 10, 50, \text{None}\}$, min split $\in \{10, 50\}$.
- **Dynamic DeepHit:** RNN hidden units $\in \{50, 100\}$, fully connected hidden layers $\in \{(100, 100), (100, 100, 100)\}$, loss parameter $\sigma \in \{1, 3\}$, learning rate $\in \{10^{-4}, 10^{-3}, 5 \times 10^{-3}, 10^{-2}\}$.
- **Joint model:** standard deviation of the Normal prior on the association parameter, $\alpha \sim \mathcal{N}(0, \sigma_\alpha^2)$ with $\sigma_\alpha \in \{10^{-6}, 10^{-3}, 10^{-1}\}$.

Recall from Appendix C.2.1 the representations of the features ϕ . For all classifier-based dynamic models (MITRA, TabPFN, and XGBoost), we tune how temporal information is encoded in the input features using two binary hyperparameters:

- `quantile_info`: whether the index of the prediction horizon is included as an additional covariate;

⁸<https://scikit-learn.org/stable/modules/generated/sklearn.impute.SimpleImputer.html>

- `time_since`: whether the time elapsed since the most recent observation prior to the timepoint t_k is included as a covariate.

Each binary flag takes values in $\{0, 1\}$, so there are four combinations of feature representations. For XGBoost, we additionally tune the tree ensemble parameters: `n_estimators` $\in \{100, 200\}$, `learning_rate` $\in \{0.1, 0.3\}$, and `max_depth` $\in \{3, 6\}$.